J Seismol (2009) 13:449–478
DOI 10.1007/s10950-008-9138-7

ORIGINAL ARTICLE

Probabilistic seismic hazard assessment of Switzerland: best estimates and uncertainties

Stefan Wiemer · Domenico Giardini · Donat Fäh · Nicholas Deichmann · Souad Sellami

Received: 8 July 2005 / Accepted: 8 September 2008 / Published online: 15 October 2008

Abstract We present the results of a new generation of probabilistic seismic hazard assessment for Switzerland. This study replaces the previous intensity-based generation of national hazard maps of 1978. Based on a revised moment-magnitude earthquake catalog for Switzerland and the surrounding regions, covering the period 1300–2003, sets of recurrence parameters (a and b values, M_{max}) are estimated. Information on active faulting in Switzerland is too sparse to be used as source model. We develop instead two models of areal sources. The first oriented towards capturing historical and instrumental seismicity, the second guided largely by tectonic principles and expressing the alterative view that seismicity is less stationary and thus future activity may occur in previously quiet regions. To estimate three alternative a and b value sets and their relative weighting, we introduce a novel approach based on the modified Akaike information criterion, which allows us to decide when the data in a zone deserves to be fitted with a zone-specific b value. From these input parameters, we simulate synthetic earthquake catalogs of one-million-year duration down to magnitude 4.0, which also reflect the difference in depth distribution between the Alpine Foreland and the Alps. Using a specific predictive spectral ground motion model for Switzerland, we estimate expected ground motions in units of the 5% damped acceleration response spectrum at frequencies of 0.5–10 Hz for all of Switzerland, referenced to rock sites with an estimated shear wave velocity of 1,500 m/s^2 in the upper 30 m. The highest hazard is found in the Wallis, in the Basel region, in Graubünden and along the Alpine front, with maximum spectral accelerations at 5 Hz frequency reaching 150 cm/s^2 for a return period of 475 years and 720 cm/s^2 for 10,000 years.

Keywords Seismic hazard · Seismicity rates · PSHA · Seismotectonics · Switzerland

Electronic supplementary material The online version of this article (doi: 10.1007/s10950-008-9138-7) contains supplementary material, which is available to authorized users.

S. Wiemer (✉) · D. Giardini · D. Fäh · N. Deichmann · S. Sellami
Swiss Seismological Service,
Institute of Geophysics, Sonneggstrasse 5,
ETH Zurich, NO, 8092 Zurich, Switzerland
e-mail: stefan.wiemer@sed.ethz.ch
URL: http://www.seismo.ethz.ch

1 Introduction

1.1 History of seismic hazard assessment in Switzerland

Probabilistic seismic hazard assessment (PSHA) is widely considered as seismology's most valu-

able contribution to earthquake hazard assessment (Abrahamson and Bommer 2005; Frankel 1995; Giardini et al. 1999; Reiter 1991; Woo 1996). Estimating the chance of strong ground motion at a given level is the most critical input for seismic zoning and building code design and is commonly done for all countries worldwide. It is also common that PSHA is periodically reviewed in order to incorporate novel data and to improve scientific understanding (Frankel 1995; Frankel et al. 1997b). Seismic hazard is assessed by combining the history of past earthquakes with the knowledge of the present seismotectonic setting and the local properties of the waves generated by earthquakes. The assessment of seismic hazard is the first step in the evaluation of seismic risk, obtained by combining the seismic hazard with vulnerability and value factors (type, value and age of buildings, as well as infrastructure, population density, and land use).

A number of studies related to hazard assessment in Switzerland have been performed in the past three decades:

- In 1978, Sägesser and Mayer-Rosa (1978) published the first PSHA for Switzerland. The hazard was based on the historical catalog available at the time, which contained epicentral intensities, I_o, as quantification of size. To compute hazard, an intensity-based attenuation function was used. Hazard was computed based on the Cornell–McGuire approach (Cornell 1968) with a zoning model of about 20 zones, which, to a large degree, mirrored the spatial distribution of seismicity. This study produced the input for the Swiss building code (SIA code 160) as well as for critical facilities, such as nuclear power plants and large dams.
- In 1995, a comprehensive study by Rüttener (1995), based on a historical parametric method, estimated the hazard and associated uncertainties at 12 sites within Switzerland. The computed parameter was again macroseismic intensity.
- Grünthal et al. (1998) significantly updated the hazard map and provided a harmonized assessment between Germany, Austria, and Switzerland (D-A-CH). The D-A-CH map was used as test region for Global Seismic Hazard Assessment Program (GSHAP) region 3 (Grünthal 1999), which represented the first unified seismic hazard model for Northern Europe (north of 46° latitude), including the majority of Switzerland. To express epistemic uncertainty in ground motions modeling, Grünthal (1999) used three attenuation relationships with equal weight: Ambraseys et al. (1996), Boore et al. (1997), and Sabetta and Pugliese (1996).
- In 2002, the Seismotectonics and Seismic Hazard Assessment in the Mediterranean Region project (SESAME; IGCP Project 382) published a first unified seismic hazard model for the entire European–Mediterranean region (Jiménez et al. 2003). For the SESAME computations, Ambraseys et al. (1996) attenuation relationships in terms of peak ground acceleration and spectral acceleration were applied. For Switzerland, the zonation of the GSHP test region 3 (Grünthal 1999) was adopted with minor modification to the southernmost source zones.

Starting in 1998, the SED initiated a number of complementary studies in view of a new generation of PSHA for Switzerland. Several doctoral theses were targeted towards improving individual elements of a forthcoming PSHA. A region-specific attenuation model for Switzerland was developed by Bay et al. (2003, 2005). The seismotectonic framework of Switzerland was assessed using focal mechanisms for stress tensor inversion (Kastrup 2002; Kastrup et al. 2004). The seismicity database was vastly improved through a series of studies devoted to paleoseismologic, historical, and instrumental seismicity (Becker et al. 2002; Meghraoui et al. 2001; Schwarz-Zanetti et al. 2003). A major result of these studies, a new moment-based earthquake catalog for Switzerland, was published in 2003 (Fäh et al. 2003; Braunmiller et al. 2005). All of these studies represent the essential groundwork for the new national PSHA of Switzerland. In this paper, we described the generation of the PSHA model, present and interpret the final hazard results, and perform sensitivity analysis.

Starting in 2002, the Swiss Nuclear Industry supported the PEGASOS project aimed at a re-assessment of the seismic hazard at the sites of the four nuclear power plants, which are located in the foreland of Switzerland (Abrahamson et al. 2002). This SSHAC level 4 (Budnitz et al. 1997) PSHA study involved multiple expert panels on source characterization, ground motion scaling, and site effect characterization. The study was completed in 2005 and has spawned numerous research papers (e.g., Cotton et al. 2006; Scherbaum et al. 2004, 2005, 2006; Bommer et al. 2004, 2005) as well as significant discussion on its interpretation (e.g., Klügel 2005, 2007; Musson et al. 2005). It is now being followed up by a refinement study to address open questions and research needs identified in the initial study. Because the Swiss National Hazard model presented in this paper was largely completed before the conclusion of the PEGASOS study, and because site-specific projects and regional hazard mapping work under somewhat different constraints, we will only briefly comment on the similarities and differences between the two studies.

1.2 Seismotectonic framework of the study region

Switzerland contains several distinct geological and seismotectonic regimes related to the collision of the African and the European plates. In terms of crustal strain rate and seismicity rate, Switzerland is located in the transition zones between areas of high seismic activity (Greece, Italy) and areas of low seismic activity (Northern Europe). The country can be subdivided into three main tectonic units (Fig. 1): (1) The Alpine belt in the south, (2) the Jura in the north, and (3) the Molasse basin in between (e.g., Trümpy 1985; Hsü 1995; Pavoni et al. 1997). Small to moderate but persistent seismic activity occurs beneath the Alpine belt and north of the Alps, including the

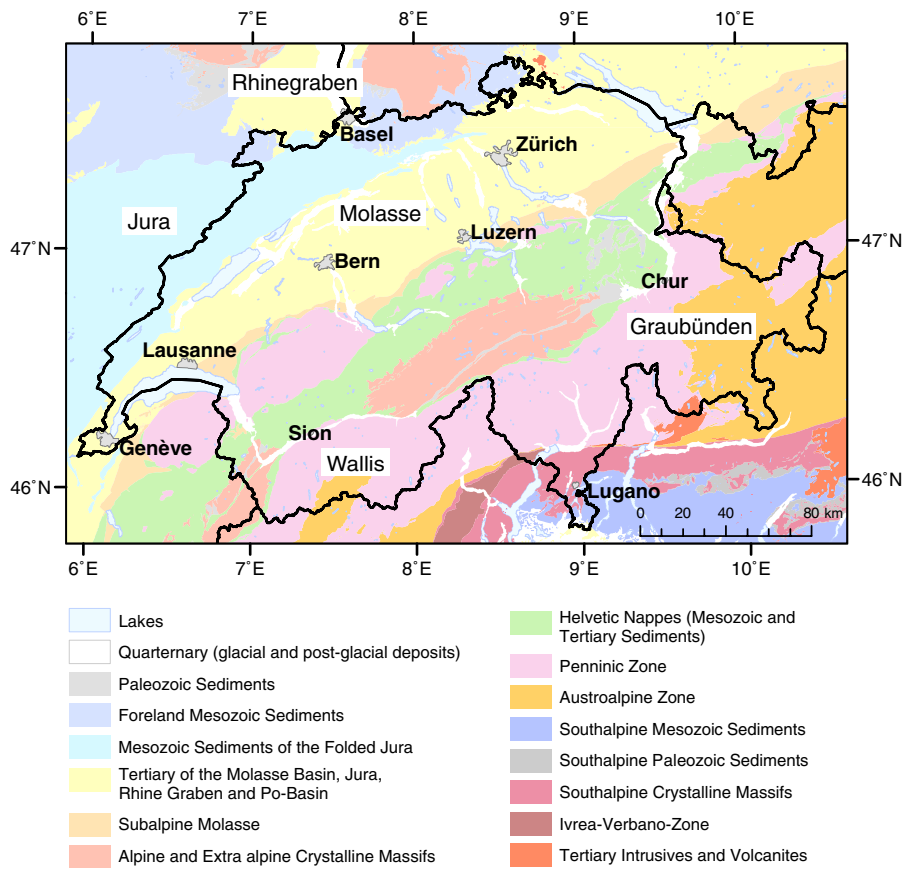

Fig. 1 Seismotectonic map of Switzerland and surrounding region. Shown are the major tectonic/geological units differentiated by color. See legend for detail

Molasse basin, the Rhine Graben, and the Jura (e.g., Deichmann et al. 2000).

A systematic analysis of 138 focal mechanisms in Switzerland and its surroundings showed that the style of faulting and the orientation of the stress field vary significantly both along strike and across the Alps (e.g., Kastrup 2002; Kastrup et al. 2004). Whereas strike-slip mechanisms with a normal faulting component dominate in the Northern Alpine Foreland and some shallow thrust mechanisms are observed along the Northern Alpine Front, the Penninic domains of the Wallis and Graubünden are characterized by normal faulting with extensional axes at a high angle to the strike of the Alps. In the Northern Foreland, the stress tensor reflects the large-scale convergence of Africa and continental Europe, with a maximum horizontal stress axis that rotates from east to west so as to remain roughly perpendicular to the Alpine arc. Thus, the least compressive stress in the northern foreland is roughly parallel to the Alpine front. Across the Alps, the variation in azimuth of the least compressive stress is defined by a progressive counterclockwise rotation of about 45° from the Foreland in the north across the Helvetic domain to the Penninic nappes in the southern Wallis. This apparent rotation of the stress field can be explained by the superposition of a local uniaxial deviatoric tension on the large-scale regional stress. The tensile nature and orientation of this local stress component is consistent with the spreading stress expected from lateral density changes due to the crustal root beneath the Alps (Kastrup et al. 2004). These results represent important input for the definition of seismic source zones.

1.2.1 Historical observations of seismicity

The bulk of our knowledge of past seismicity relies on the historical record of earthquake damage. From these macroseismic observations, we derive approximate locations and magnitudes of past events. On average, 10–15 earthquakes are felt each year within Switzerland; damaging events are expected every 5–10 years. Over the past 800 years, a total of 28 events of a moment

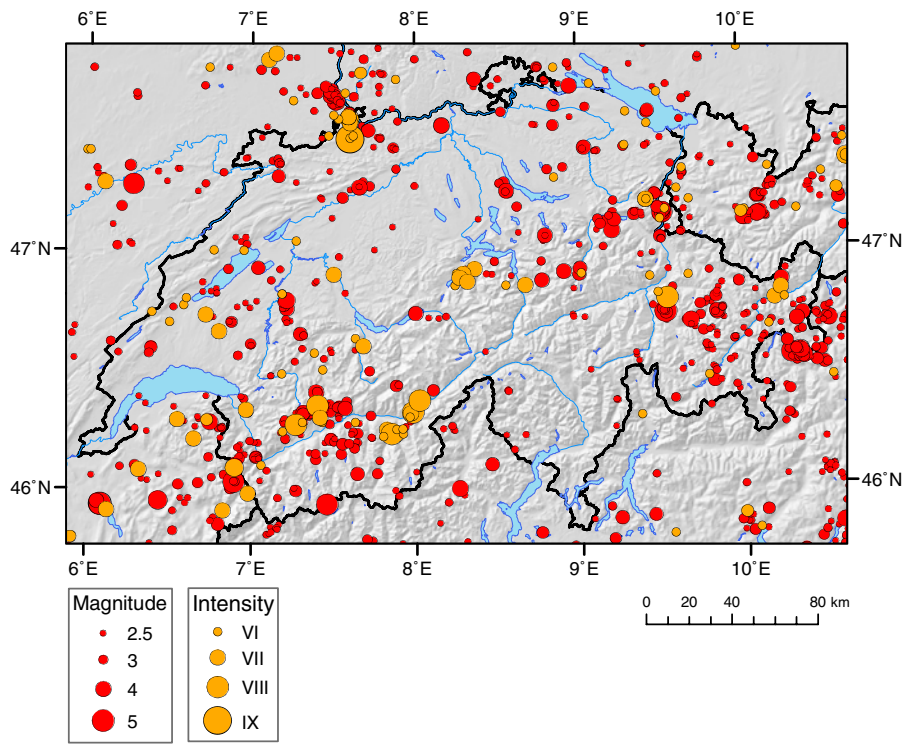

Fig. 2 Map of Switzerland. *Orange circles* mark epicenters with epicentral intensity $I_x > \text{VI}$ since the year 1300, based on macroseismic observations (Fäh et al. 2003). *Red circles* show the instrumentally recorded events with $M_L > 2.5$ in the period 1975–2007

magnitude $M_w \geq 5.5$ are known to have occurred. A map of all events known to have caused damage to buildings (macroseismic intensities $\geq$ VI) is shown in Fig. 2 (top). Twelve of them reach an intensity of VIII or higher, causing severe damage. Destructive earthquakes of intensity IX or larger have occurred in the past, but their return periods exceed 1,000 years (Fäh et al. 2003; Meghraoui et al. 2001). The highest seismic activity is observed in the region of Basel and in the Wallis. Other regions of enhanced activity are central Switzerland, Graubünden, and the Rhine Valley of St. Gallen.

The earthquake that occurred on October 18, 1356 in the region of Basel is the strongest historically documented earthquake in central Europe (Fäh et al. 2003). A repeat of this event has been estimated to cause damages on the order of several tens of billions of Swiss Francs to buildings alone, as well as hundreds to thousands of fatalities.

1.2.2 Instrumental observations of seismicity

Instrumental observations complement the macroseismic observations for larger events and are the basis for a homogeneous record of the seismicity in Switzerland since 1975. With the exception of central Switzerland, which has shown little activity since the earthquake sequence of Sarnen in 1964, and of the recent lack of activity in the Oberwallis, the instrumentally recorded seismicity of the last 29 years (Fig. 2, bottom) is concentrated in the same regions as the seismicity derived from the historical record (Fig. 2, top).

An important factor for the PSHA, which can be derived only using instrumental recordings, is the hypocentral depth of earthquakes. However, the routinely determined depth of earthquakes in Switzerland is poorly constrained for many events. Therefore, we rely on results from dedicated studies such as Deichmann et al. (2000) and Husen et al. (2003). The results of Deichmann et al. (2000) are based on high-quality locations of selected well-recorded events. Husen et al. (2003) also derived a three-dimensional velocity model and used a nonlinear location algorithm (Husen et al. 2003; Lomax et al. 2001) to further constrain depth and its uncertainty. Both studies consistently show a major difference in depth distribution between the Alps proper and the Northern Foreland (Jura, Molasse): Deeper earthquakes (mean depth = 13 km, maximum depth > 30 km) occur only in the north beneath the Molasse Basin, whereas in the south under the Alps where the crust is up to 55 km thick, earthquakes are restricted to the upper 10–15 km (mean depth = 7 km; e.g., Deichmann et al. 2000). This major difference across the Alpine Front is one of the principle design criteria used for our seismic source zonation.

1.2.3 Paleoseismic investigations in central and northern Switzerland

Since 1997, a number of investigations have been undertaken with the aim of identifying paleoseismological approaches suitable for application in northern and central Switzerland and to reconstruct the Late Pleistocene and Holocene record of strong earthquakes (Becker and Davenport 2003; Becker et al. 2002; Schnellmann et al. 2002, 2004). These results change our understanding of the earthquake record in northern and central Switzerland and of how earthquakes affect the geological record. Most relevant for our study are the investigations related to the Rheinach fault near Basel, now believed to have been also the source of the 1356 Basel event (Meghraoui et al. 2001). Paleoseismologic studies (Meghraoui et al. 2001; Becker et al. 2002) suggest that similar size events have indeed taken place on the Reinach fault. There is evidence for at least three earthquakes, which occurred on that branch of the fault within the last 8,500 years with vertical displacements ranging from 0.5 to 0.8 m.

Analyzing multiple subaqueous landslide deposits in Lake Zurich and Lake Lucerne through high-resolution seismic surveys and radiocarbon-dated sediment cores, Strasser et al. (2006) identified evidence for three large paleo-earthquakes in central Switzerland with moment magnitudes ($M > 6.5$–7.0). These magnitudes significantly exceed the historically known values. These earthquakes occurred during the past 15 ky and were strong enough to simultaneously affect a large region that includes the present-day major cities of Lucerne and Zurich.

1.2.4 Active faults and deformation in Switzerland

Knowledge of active faults and of deformation rates on such faults is very limited in Switzerland. Whereas numerous faults are identified on geological maps at all scales, these do not correlate with observed seismicity. In the literature, there is no convincing evidence for Quaternary movements that has offset topography and post-glacial features (e.g., Eckardt et al. 1983). However, within the generally rather diffuse epicenter distribution, two epicenter lineaments have emerged in recent years, which seem to be related to active faults at depth within the crust. The first is an almost rectilinear 20- to 30-km-long north–south striking epicenter alignment east of the city of Fribourg. Based on the good agreement with the focal mechanisms, with the subsurface structures identified in reflection seismic experiments and in geomagnetic studies, as well as with morphological features of the region, it could be demonstrated that the earthquake lineament of Fribourg corresponds to an active fault zone capable of hosting a possible M6 event (Kastrup 2002; Kastrup et al. 2007). The second lineament is a narrow earthquake zone that is located along the northern border of the Rhone Valley in the Wallis and that possibly extends in a southwestern direction all the way into the Haute-Savoie. The northern Wallis segment of this epicenter alignment is probably a long-lasting consequence of the 1946 earthquake sequence of Sierre. However, in recent years, an increase of activity southwest of this region suggests the possible existence of an active fault zone whose dimensions could accommodate an earthquake considerably larger than what is known to have occurred previously. Ongoing investigations, such as the precise relative locations of events in individual sequences within the larger earthquake zone, will contribute towards clarifying this issue.

Due to the low deformation rates, detailed geodetic measurements for individual faults do not exist in Switzerland to date. However, geodetic deformation rates help to define broad regional differences in seismic potential. In Switzerland and in neighboring areas, geologically estimated deformation rates are homogeneous and are overall very low, consistent with recent GPS measurements. The average total convergence rate between Africa and Europe for the past 49 Mya was about 0.9 cm/year (Regenauer-Lieb and Petit 1997), which is in good agreement with the rate of 0.94 cm/year for the past 3 Mya, as given by NUVEL-1 (DeMets et al. 1990). These numbers are reasonably consistent with long-term geological strain rates. Vertical movements are too small to distinguish isostatic signals due to post-glacial rebound from tectonic signals.

2 Input for PSHA in Switzerland

Input parameters needed for performing a PSHA following the Cornell–McGuire approach (Cornell 1968; McGuire 1976; Reiter 1990) are:

1. An earthquake catalog, which is used to derive recurrence rates and to estimate the maximum possible earthquake for each source zone.
2. A seismotectonic source model, which defines fault or areal zones of equal seismic potential.
3. A predictive ground motion model (PGMM), which describes the attenuation of amplitudes (acceleration, velocities) as a function of distance and the scaling with magnitude. Individual models are constructed for different frequencies and local site conditions.

Below, we describe how these input parameters were derived for Switzerland.

2.1 Earthquake catalog of Switzerland

The historical earthquake catalog and macroseismic database for Switzerland were revised during the period 1998–2003 (Fäh et al. 2003). The resulting Earthquake Catalog of Switzerland (ECOS), covering also the border regions, integrates information from different sources: (1) the Macroseismic Earthquake Catalog of Switzerland (MECOS 02) with events since 250; (2) the annual reports of the Swiss Earthquake Commission since 1879; (3) the epicenter locations of the Swiss Instrumental Network since 1975; and (4) additional information from 12 earthquake catalogs of neighboring countries and international agencies. The ECOS catalog can be downloaded from www.seismo.ethz.ch, along with a detailed

report describing its compilation. Note that some of the events of the twentieth century were independently reappraised by Ambraseys (2003); however, because this reappraisal is not internally consistent with the remainder of the ECOS approach, we did not use this catalog for our PSHA.

Moment magnitude, M_w, was chosen as measure of earthquake size for both the historically known and the instrumentally recorded events. This involved a reassessment of instrumental magnitudes in order to standardize the various types of magnitude scales and the different measurement procedures of various institutions to a common basis (Braunmiller et al. 2005). Then, a set of calibration events with values of intensity as well as magnitude was established. This calibration set was used to assign a magnitude value to the historical earthquakes. In case of larger events, the magnitude assessment is based on an analysis of the entire macroseismic field according to the method of Bakun (Bakun and Wentworth 1999; Wesson et al. 2003). For smaller events, magnitudes are computed from epicentral intensities using an empirical relationship (Fäh et al. 2003). After removal of all events identified as explosions and of all events judged to be uncertain, ECOS comprises a total of about 20,000 earthquakes. Figure 3 shows a time–magnitude plot of the entire ECOS database since 1300. Note that magnitude 2–4 events are binned in 0.3 magnitude intervals before 1970 as a result of the conversion from epicentral intensity to magnitude.

2.2 Definition of seismic source zones

The assessment of seismic hazard requires the interpretation of past seismicity and tectonic knowledge to forecast likely locations of future shaking. Several methods have been proposed, but there is no ideal and proven way to derive a set of seismic source zones; zoning remains inherently a matter of expert judgment. It is therefore important to capture and propagate the uncertainty of any zoning model.

Seismotectonic zoning is intrinsically linked to the question of stationarity in space and time. Will future seismicity follow the pattern of the past? Will areas which were active in the last centuries remain active also in the next 50–100 years (Fig. 2)? Or have areas of past seismicity currently exhausted their potential and will remain quiet while other areas will become more active? These issues are critical in areas of spatially dispersed seismicity such as Switzerland because the lack of knowledge of active faulting requires the use of areal sources as the primary zoning tool. We decided not to use faults as linear or areal source zones because only very limited information is available for Switzerland and the known seismic activity along these faults is, in our opinion, insufficient to characterize them as source zones. Doing so would introduce a bias in the hazard assessment because the information density on known faults is so sparse, and therefore, few selected areas would receive a ‘special’ treatment. Areal sources can be either used to closely trace

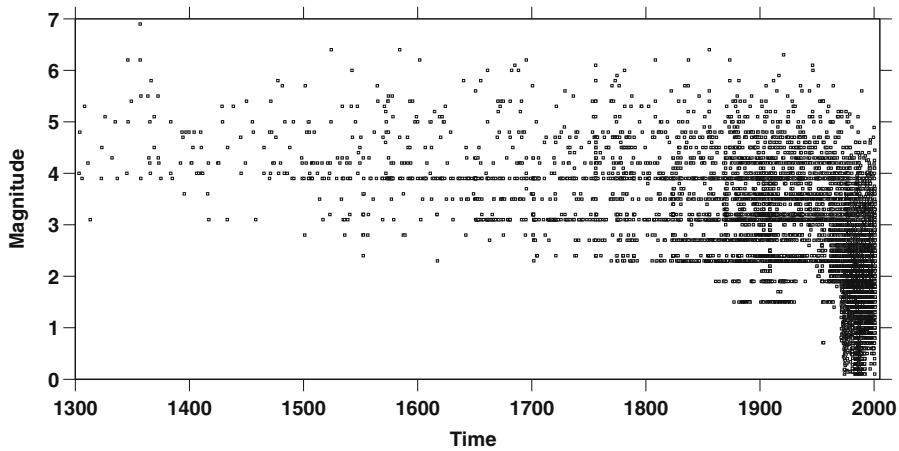

Fig. 3 Time–magnitude distribution of the events in the ECOS database

the historical seismicity, or they can be used to also reflect seismotectonic knowledge. In the latter case, the activity in an area could spread with the same probability to a neighboring area of identical seismotectonic character. As an alternative, smoothed seismicity models have been used in some hazard studies (Frankel 1995; Rüttener et al. 1996; Woo 1996) to distribute historical seismicity over a larger region. These models generally use a constant smoothing kernel across the entire region, thus avoiding potential bias. Their disadvantage is that they ignore existing boundaries and do not allow for the integration of external knowledge and that the choice of a smoothing parameter is likewise subjective.

For our hazard computations, we developed two models of areal sources. Model 1 (SEIS) is mostly driven by historical seismicity; model 2 (TECTO), using generally larger zones, attempts to capture the major tectonic features of the region. For the peripheral regions around Switzerland, we relied largely on the existing source models that were developed previously for the international hazard mapping projects GSHAP and SESAME (Grünthal 1999; Jiménez et al. 2003). The geometry of the two source zone models is plotted in Fig. 4. We feel that the TECTO model represents well alternative scenarios that assume that the seismicity of the next years changes from what has been observed as persistent clusters of activity in the past 1,000 years (Fig. 2). However, we assume that such a change is an unlikely scenario, which is why we only give a 10% weight in the logic tree branch to the TECTO model.

Below, we describe some of the major tectonic features and resting zoning decisions for the study region.

Helvetic Front This is the major tectonic separation between the Alpine Foreland and the Alps proper and introduced as a single arched zone in model TECTO (Fig. 4, zone 4) and subdivided into an eastern and western arc in model SEIS (Fig. 4, zones 4 and 24). Its definition is based on: (1) the depth distribution of the hypocenters (Deichmann 1992; Deichmann et al. 2000), (2) geological information, and (3) density of the seismic events. The Helvetic Front is shown on any geological map (e.g., Trümpy 1985). It is characterized by different lithologies with different rheological/mechanical properties to the south and north. The tectonic contact zone of the Helvetic Front dips towards the south at an angle of 30° to 45°. The seismic activity along the Helvetic Front is apparently

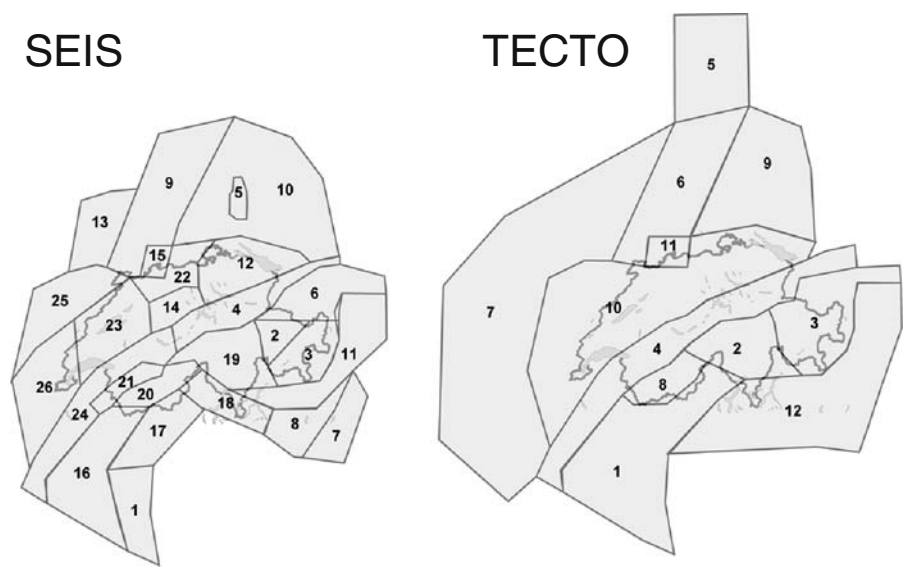

Fig. 4 Maps of Switzerland. *Left*: source zones of model 1, SEIS, which is largely based on the historical seismicity. *Right*: source zones of model 2, TECTO, which assumes that the seismicity follows broad tectonic regions. The corresponding names, recurrence parameters, completeness estimates, and zone geometries are given in the Electronic Appendix

contained within the Alps proper rather than in the foreland (Fig. 2). Given that the seismo genic crust is constrained to be at most 20 km thick underneath the Alps, in contrast to the more than 30 km seismogenic thickness to the north (Deichmann et al. 2000; Husen et al. 2003), a broad thermal anomaly (Jaboyedoff and Pastorelli 2003) might govern the depth distribution of seismicity. Alternatively, the seismic activity in the lower crust beneath the northern Alpine foreland and thus the lower resistance to brittle failure might also be a consequence of increased fluid pressure (Deichmann 1992).

Insubric Line The Insubric (also called peri-Adriatic) lineament is a major fault separating the alpidic overprinted central Alps in the north from the Southern Alps, which where hardly affected by alpidic metamorphism. It is a sharp and nearly vertical contact. A wealth of data provides several lines of evidence for different crustal characteristics on both sides of this fault. The Southern Alps were built on the Adria (Italy) microplate, whereas the central Alps derive from continental fragments that either belonged to the southern margin of Europe or were isolated within the Tethys Ocean before collision between Adria and Europe (e.g., Schmid and Kissling 2000). Geophysical information including reflection seismology (Kissling 1993; Schmid et al. 1997; Ye et al. 1995), seismic behavior (less active towards the south), gravimetery, and Moho depth (Waldhauser et al. 1998) confirm the geological differences. The Insubric lineament is introduced only in model TECTO (Fig. 4, boundary between zone 12 and zones 1, 2 and 3), whereas in SEIS, its contribution to seismic activity is considered negligible.

Jura The Jura region is separated from other regions on the basis of rock composition and the existence of a shallow-dipping contact zone between the deformed sedimentary cover and the apparently less deformed basement (pre-Triassic rocks; e.g., Burkhard 1990; Sommaruga 1999; Truffert et al. 1990). The Jura region is separated from other source zones in SEIS (Fig. 4, zones 22, 23, 25 and 26), while it is combined with the Molasse in TECTO (Fig. 4, zone 10).

Southern Rhinegraben The major structural element cutting the European lithosphere is characterized by sparse, sometimes destructive seismicity (Fig. 4 zones 9 and 15 in SEIS, zones 5, 6, and 11 in TECTO). This activity has been more pronounced in the southern part where the graben intercepts the Jura folds. To incorporate the Rhinegraben activity, we define in both models a wide north–south trending zone that includes the Rhinegraben and its shoulders. In principle, the Rhinegraben could be further subdivided into a northern and a southern part along the Variscan suture zone (Lalaye-Lubine Fault from the Vogeses to Baden-Baden in the Black-Forest, the Erstein Sill below the sedimentary infill of the Rhinegraben; Villemin et al. 1986; Sissingh 1998; Burg et al. 1994); however, because this region is far from our study area, we did not do so. In both models, however, we define a specific Basel source zone (Fig. 4, zone 15 in SEIS and zone 11 in TECTO), which contains the Basel activity of the historical and paleoseismic record. We feel that this subdivision is justified because this segment, while tectonically similar to the remainder of the Rhinegraben, has persistently produced more activity in the past and is in our assessment likely to continue to do so in the future.

Swaebian Alb The Swaebian Alb is a documented zone of episodic activity with consistent strike-slip focal mechanism oriented in a north–south direction. The Swaebian Alb is characterized as a specific source zone in the SEIS (Fig. 4, zone 5) model only.

The focal depth of earthquakes is an important input to PSHA not only for defining source zones but also for ground motion predictions. Based on the high-precision relocations of Deichmann et al. (2000) and Husen et al. (2003), we assign two different depth distributions for events north and south of the Alpine Front. We did not, however, feel that the data allow us to further subdivide the regions based on focal depth.

2.3 Estimation of recurrence parameters

2.3.1 Data completeness with time

To model the seismicity in each zone, we need knowledge on the magnitude of completeness, M_c, below which only a fraction of all events in a magnitude bin are detected by the network (Kijko and Graham 1999; Rydelek and Sacks 2003; Wiemer and Wyss 2000, 2003). Completeness as a function of space and time in the ECOS catalog varies, first of all, country-by-country because the different countries use different methods to compile the catalogs. Completeness estimates for historical datasets are largely a matter of expert judgment based on an evaluation of various plots of the seismicity. This iterative process leads to a definition of completeness periods through time for each country. Results are then checked against historical estimates of completeness, as given in the ECOS catalog. For Switzerland, an independently derived estimate of completeness based on a historian's estimate of data source availability can also be consulted (Fäh et al. 2003). For the instrumental data, completeness is also computed using an algorithm developed for completeness mapping (Wiemer and Wyss 2000).

Because sources cross national borders, and because even within individual countries differences in M_c for different time periods are apparent, we interactively review the normalized cumulative frequency–magnitude distribution of events for each source zone. In some cases, we adjust the completeness threshold.

Completeness estimation, especially for historical data, is subject to large uncertainties. To express these uncertainties and to allow for the fact that historical data for low magnitudes are less reliable, we define an additional alternative model 2 with a higher M_c cutoff. This alternative model 2 results in relatively higher weights to the recent earthquakes in the instrumental dataset. We thus have two completeness models for each source region. The final determined M_c thresholds for each source zone of models TECTO and SEIS are given in the Electronic Appendix to this publication.

2.3.2 Explosion contamination

The ECOS catalog contains a number of unidentified explosion events. Despite the best efforts of network operators to identify these events, it is common in all regional earthquake catalogs to have such unidentified events because the separation of explosion events from tectonic ones is difficult (Fäh and Koch 2002; Koch and Fäh 2002; Wiemer and Baer 2000; Wüster 1993). These events are mainly limited to the most recent 30-year period of data. Their magnitudes are believed to be mostly smaller than $M_w = 2.5$; however, these small events have the potential to significantly bias the a and b value computation in some regions, especially because the size distribution of explosions is generally much steeper (higher b values) than of tectonic earthquakes (Wiemer and Baer 2000). To estimate the number of unidentified explosions, we plot a histogram of the time of the day of all events not marked as explosion in the ECOS database. This plot reveals a typical pattern for a quarry-blast-rich region (Wiemer and Baer 2000): Detection is best in the nighttime hours (Rydelek and Sacks 1989); in other words, M_c is lower. A peak during daytime hours around 12 UTC, however, is not explained by improved completeness, but caused by artifacts. Based on the hourly histogram, we estimate that the ECOS catalog contains roughly 500 explosions.

To further investigate these explosions, we map the ratio of nighttime-to-daytime number of earthquakes, R (Wiemer and Baer 2000). The map in Fig. 5 was computed using sampling volumes of 60 events. Ratios of $R > 2$, plotted in blue to purple colors, show a statistically significant (as compared to a uniform probability density function) increased seismicity during daytime hours and are indicative for the presence of quarry blasts. On the other hand, statistically significant low ratios (red colors in Fig. 5) could also be indicative of man-made activity (e.g., nighttime underground mining activity). However, their interpretation is less reliable because they show the same trend as the aforementioned daily variations in M_c due to daytime noise. An example of the hourly distribution of events in an anomalous

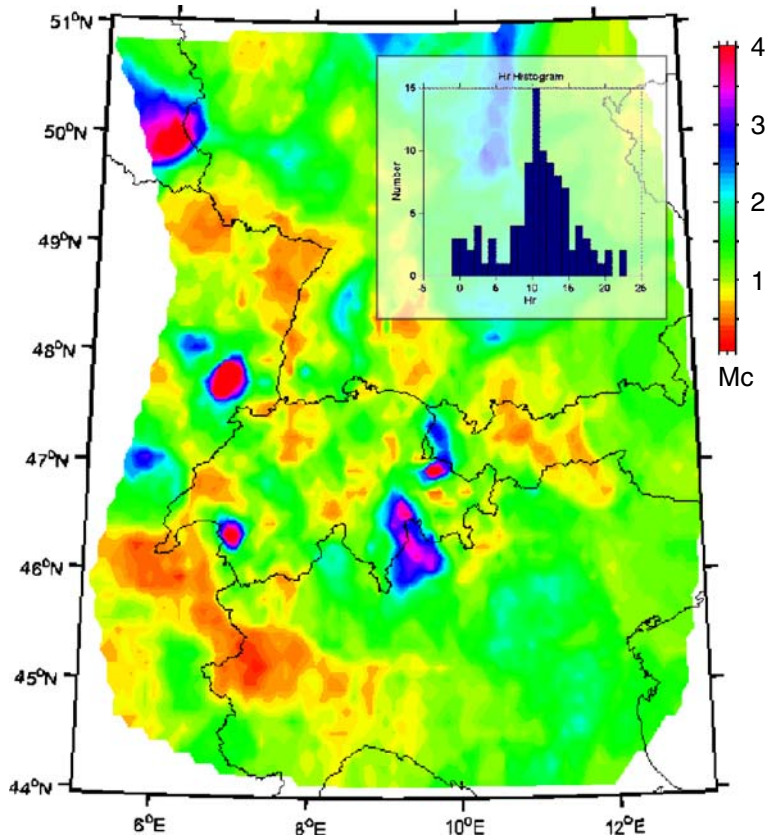

Fig. 5 Map of Switzerland and its surrounding regions. Color-coded is the daytime to nighttime ratio of events (daytime, 800–1800 GMT). High ratios (*blue to purple colors*) suggest the presence of explosion contamination in the data. The frame above shows the histogram of the hourly distribution of events located near the "Wallis anomaly"

region is shown in the inset in Fig. 5. To remove the explosion contamination, we follow the iterative approach outlined in Wiemer and Baer (2000). The final "dequarried" catalog contains fewer earthquakes during daytime hours because inevitably some daytime tectonic earthquakes are also removed. However, because the removed real event set is independent of magnitude scaling, and presumably follow the true natural size distribution, the effect is only a minor reduction in activity rate for these volumes. It is also limited to the instrumental data. This unavoidable rate reduction is considerably less biasing than the original bias in rate and *b* value caused by the explosions. In an additional step, we also removed manually events near a mining area in France (6.8° W, 49.4° N). This region shows an anomalously low daytime to nighttime ratio and a peculiar time distribution and magnitude size distribution of events. The numerous events in this region after 1980 correspond almost entirely to mining related activity (J.P. Burg 2002, personal communication).

2.3.3 Declustering the ECOS catalog

Declustering attempts to separate the time-independent part of seismicity (background) from the time-dependent or clustered parts (aftershocks, foreshocks, and swarm type activity). For most hazard-related studies, it is required that the seismicity behaves in a time-independent fashion (Reiter 1990; Giardini 1999; Frankel 1995). Working with the time-independent dataset (from now on called "declustered") avoids biasing the average rate assessments with data from, for example, prominent aftershock sequences that may not be representative of the average behavior of a crustal volume. We test whether or not the temporal distribution of events within the ECOS catalog is Poissonian (Knopoff 1964; Gardner and Knopoff

1974; Reasenberg 1985), which would argue that declustering may not be necessary. We apply a χ^2 test (Taubenheim 1969) to a variety of ECOS subsets (in space, magnitude, and time) testing for the null hypothesis: Earthquakes in the ECOS dataset are independent and follow a Poissonian distribution. For all subsets, we find that the null hypothesis can be rejected at a significance level of 99.9%. Therefore, declustering the dataset is needed.

There is no unique way to separate time-dependent earthquakes from background ones. We explored the two main declustering algorithms used in seismicity studies. The first approach was introduced by Gardner and Knopoff (1974) and has been used in numerous hazard-related studies (e.g., Frankel 1995). It simply removes a space and time window after each mainshock. We explored first of all the original parameters given in Gardner and Knopoff (1974). In addition, we apply window parameters optimized for central Europe by Grünthal (personal communication) and alternatives given by Uhrhammer (1986) and Youngs et al. (1987). The diversity of the window parameters illustrates again the non-uniqueness of declustering. The second approach we evaluated is by Reasenberg (1985) who defines interaction windows in space-time in a somewhat more sophisticated way that attempts to introduce physical properties behind triggering. The spatial and temporal extent of a cluster is not fixed, as it is in the windowing method, but depends on the development of an individual sequence. Several free parameters in Reasenberg's algorithm determine the degree of clustering that is applied. When comparing the results of the two approaches in terms of total number of identified dependent events (38.8% versus 47.7%) and in terms of their contribution to the total moment released (0.94% versus 1.99%), Reasenberg's and Gardener and Knophoff's declustering approaches vary considerably. However, sensitivity tests show that the difference in terms of resulting hazard is minor. We selected Gardener and Knophoff's approach with Grünthal's parameters as our preferred method because its parameters are optimized for central Europe and results seem to fit selected recent sequences in Switzerland.

2.3.4 Estimating seismicity rates

Various approaches have been used to estimate recurrence parameters in the past. The debated questions in this respect, despite the aforementioned issues of completeness, are related to the most appropriate way to determine a and b values (least squares, weighted least squares, maximum likelihood; see Bender 1983) and to the question to the allowed degree of spatial variability of b values. We reviewed the existing literature and found no fully satisfying approach. In light of the recently well-established spatial variability in b values (Schorlemmer et al. 2004a, b; Wiemer and Wyss 1997, 2002), we feel that using an overall constant b value, as done in many parts of the USA (Frankel et al. 1997a), is not appropriate. However, we are also uncomfortable with the sometimes large variability of b values seen in regional zonations (Giardini et al. 1999; Jiménez et al. 2003), which we believe are often statistical variations due to the small sample sizes investigated (Wiemer and Wyss 2002). The question of when a regional b value versus local ones should be used has, in our opinion, not been answered systematically before, and here, we present a new approach that integrates model selection theory for decision making.

The basic principles of our recurrence rate estimation are:

- *Objectivity and reproducibility*. The rates should be computed in an automatic fashion and reflect significant statistical measures;
- *Simplicity*. We use a simple model with few parameters unless the data require a different approach.

To achieve these goals, we develop a multi-step scheme to assess the earthquake size distribution and activity rate. We use the truncated exponential distribution, which is the earthquake recurrence relationship most commonly used in PSHA. It is derived from the Gutenberg and Richter (1944) recurrence model by truncating the rate density of earthquakes at a maximum magnitude, $M_{\max}$. Other recurrence relationships were considered but ultimately rejected because: (1) there is little evidence for the validity of different recurrence laws in the literature and

(2) faults based characteristic models badly fit the source zoning applied in our study. To estimate recurrence parameters with datasets of variable completeness with time, we use Weichert's (1980) approach and a maximum-likelihood estimator (Aki 1965; Bender 1983; Shi and Bolt 1982; Utsu 1999).

In a first step, we assess the overall b value of the region, b_0. In regional hazard studies, an overall b value is often used in order to stabilize the result by avoiding undue fluctuations of b particularly in zones of low seismicity (Frankel 1995; Frankel et al. 1997b). We use the aforementioned M_c estimates derived for each zone. From the frequency–magnitude distribution of all events within Switzerland or within 100 km of the Swiss border (Fig. 6), we can observe that the historical data, particularly for the period 1881–1975, show a higher activity rate than the instrumental data. We carefully investigated the possibility that a systematic shift in magnitude occurred between instrumental and intensity-based data (Braunmiller et al. 2005; Fäh et al. 2003); however, we could not find such evidence. In addition, we note that the shift in activity between the two periods is only present in some regions, most noticeably in the Wallis. This suggests that this shift is at least partially caused by a true, natural change in activity rate, which is well established for some regions, such as the Wallis, based on macroseismic observations.

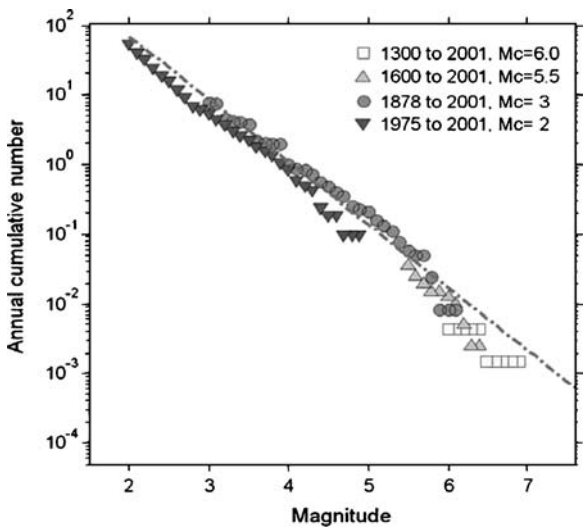

Fig. 6 Annual cumulative number of events within Switzerland and neighboring regions. The frequency–magnitude distribution is broken down into four completeness periods, as given in the legend. The *dashed gray line* represents the best fitting model to the data, with a b value of 0.90. This value is used as the regional b value, b_0

Independent of its cause, the change in activity rate causes a complication when estimating recurrence rates: If one ignores the fact that the two periods have different activity rates, or a values, then a systematic bias towards a lower b value is introduced. This forces us to consider a model that allows not just one a value but two: one for the instrumental and one for the historical data (dashed line in Fig. 6). We take its b value of 0.90 as our regional b_0 estimation. It is consistent with the slopes observed in both the historical and instrumental data for this region.

2.3.5 Assessing recurrence in each zone

The next step is to assess the recurrence parameters in each zone. Keeping with our objective to only change the overall b value when the data require (or allow) so, and also keeping in mind the possibility that the activity rates between the instrumental and historical data may differ, we design three different models of recurrence. This allows us to capture the uncertainty in recurrence rate estimation. These models are:

1. Constant $b = b_0$, variable a value determined on the entire observation period (taking into account the duration of each completeness period).
2. Variable b and a value. Here, we determine both the best fitting a and b value (in a maximum-likelihood sense).
3. Constant $b = b_0$ and two variable a values (a_1 and a_2): one for the instrumental period (1975–2000) and one for the historical period (1300–1975). The average a value is then computed as the weighted (for the period length) average of the two a values.

We then measure the relative goodness of fit of each model to the data in each zone and establish relative weights. The fit of each model to the observed data is computed as a likelihood score (Ogata 1983); however, because the models have

different degrees of freedom (i.e., free parameters), these likelihood scores cannot be compared directly. If two models have the same likelihood score, the one with fewer free parameters should be the preferred model because a simpler model tends to be more robust. To find the best fitting model, we use the corrected Akaike information criterion, AIC_c (Kenneth et al. 2002):

$$AIC_c = -2\max(\ln L) + 2(P) + \frac{2P(P+1)}{N-P-1}$$

with $\log L(a, b)$ being the log-likelihood function, P the number of free parameters, and N the sample size. In contrast to the original Akaike information criterion (Akaike 1974; Imoto 1991; Ogata 1999), the corrected AIC_c penalizes for the amount of samples, which becomes critical for small sample sizes. The AIC_c is useful in selecting the best model in the set; however, even that model may be poor in an absolute sense (Kenneth et al. 2002). The model with the lowest AIC_c is the preferred model. For most zones in our whole-Switzerland model, model I is preferred. In the Basel zone and in few other zones, a lower b value is preferred. The AIC_c can also be used to obtain weighted alternative models in order to express the epistemic uncertainties in a logic tree approach. The best model is determined by examining their relative distance to the "truth". The first step is to calculate the difference between model i and the model with the overall lowest AIC_c:$\Delta i = AIC_c(i) - \min(AIC_c)$. The relative weight can then be described as:

$$w_i = \frac{\exp(-0.5 \times \Delta_i)}{\sum_{r=1}^{R} \exp(-0.5 \times \Delta_r)}$$

where w_i are known as Akaike weights for model i and the denominator is simply the sum of the relative likelihoods for all candidate models.

In Fig. 7, we show the fit of the three models and their relative weights for eight zones, taken from the SEIS and TECTO models, and for either completeness models 1 or 2. Note that in some cases, all three models give almost identical results, while in others, the three models differ significantly. All recurrence estimates and weights are given in the Electronic Appendix.

Fig. 7 Examples of the rate estimation for eight zones from the SEIS and TECTO models. The recurrence parameters, AIC_c scores, and estimated weights are given at the *bottom of each frame*

2.3.6 Maximum possible earthquake

The choice of the maximum possible earthquake, M_{max}, might have a considerable influence on the hazard, especially at longer return periods. M_{max} is possibly the most difficult recurrence parameter to assess in the study area because the physical understanding of M_{max} is poor and the database is statistically very limited. We considered several techniques for estimating M_{max} used in past hazard studies: (1) the EPRI approach (Johnston et al. 1994) based on a global database of stable continental regions; (2) regional strain-based constraints (Regenauer-Lieb and Petit 1997; DeMets et al. 1990); (3) global statistical models (Kagan 1999; Kagan and Jackson 2000); (4) seismotectonic constraints (maximum available feature; Coppersmith 1994, Wells and Coppersmith 1994); (5) Kijko's numerical approach based on observed seismicity (Kijko and Graham 1998; Kijko et al. 2001); and (6) 'one step beyond' method, which adds a constant increment to the observed maximum at each zone (e.g., Slejko et al. 1998). In our assessment, none of these provides a convincing and well-constrained answer. We therefore decided to first of all derive main guiding principles for our M_{max} determination:

- M_{max} should be relatively large because we see no evidence from worldwide studies or seismotectonic constraints that rule out M6 class events in any region of Switzerland. This kind of events may have recurrence rates exceeding 10,000 years in most zones and might not be traceable in the historical or geological record. This view is supported by the work of Strasser et al. (2006) who identified, based on lake sediments, three large ($M_w \geq 6.5$) events in central Switzerland in the past 15 ka where the historical record shows no events of similar size.
- Our M_{max} assessment should reflect the uncertainty of this parameter.

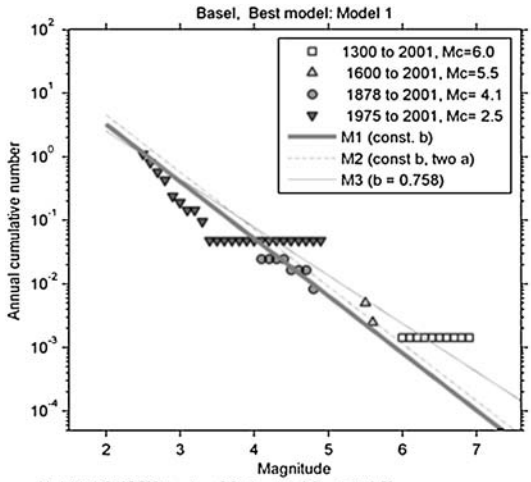

Model 1, AIC: 35.592, a-value= 2.31; b-value: 0.9, weight: 0.52
Model 2, AIC: 37.292, a-value= 2.46; b-value: 0.9, weight: 0.22
Model 4, AIC: 37.009, a-value= 1.92, b-value: 0.758, weight: 0.26

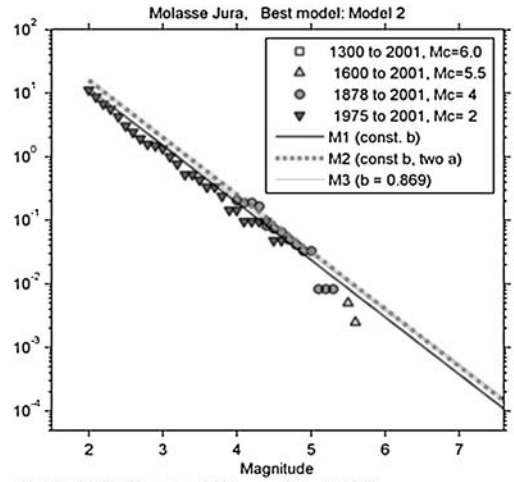

Model 1, AIC: 79.489; a-value= 2.88; b-value: 0.9, weight: 0.39
Model 2, AIC: 79.349; a-value= 3, b-value: 0.9, weight: 0.42
Model 4, AIC: 80.84; a-value= 2.81; b-value: 0.869, weight: 0.2

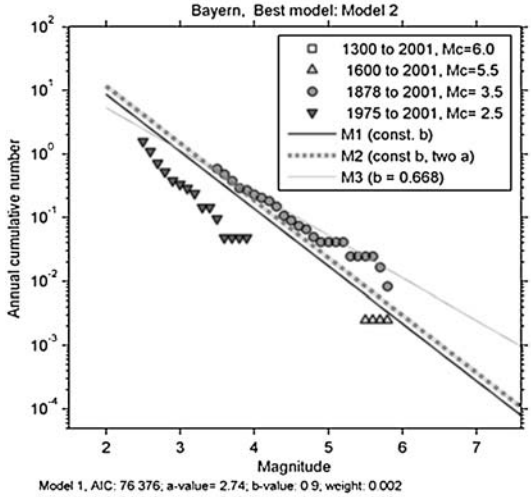

Model 1, AIC: 76.376, a-value= 2.74; b-value: 0.9, weight: 0.002
Model 2, AIC: 64.043, a-value= 2.87; b-value: 0.9, weight: 0.96
Model 4, AIC: 70.496, a-value= 2.06; b-value: 0.668; weight: 0.038

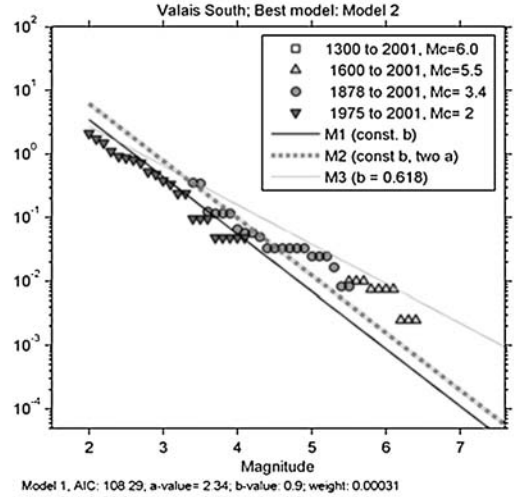

Model 1, AIC: 108.29, a-value= 2.34; b-value: 0.9; weight: 0.00031
Model 2, AIC: 92.568; a-value= 2.59, b-value: 0.9; weight: 0.8
Model 4, AIC: 95.393; a-value= 1.67; b-value: 0.618, weight: 0.2

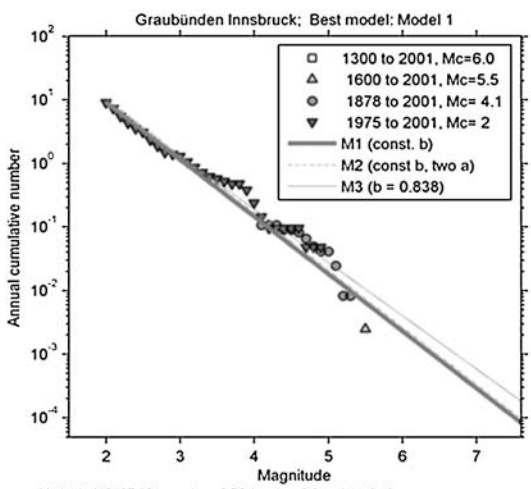

Model 1, AIC: 67.261; a-value= 2.76; b-value: 0.9, weight: 0.48
Model 2, AIC: 68.809; a-value= 2.83; b-value: 0.9, weight: 0.22
Model 4, AIC: 68.165, a-value= 2.63; b-value: 0.838; weight: 0.3

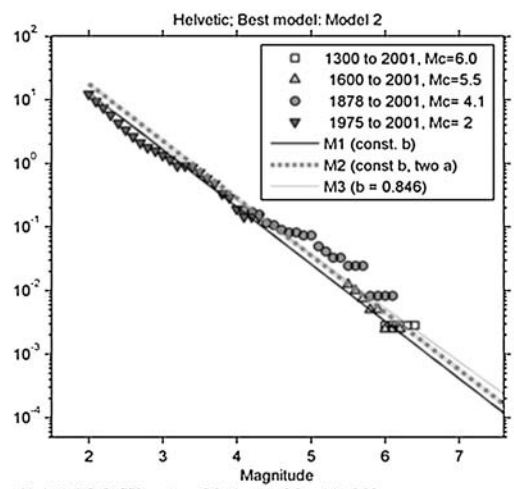

Model 1, AIC: 91.773, a-value= 2.91; b-value: 0.9, weight: 0.36
Model 2, AIC: 91.566; a-value= 3.05; b-value: 0.9, weight: 0.4
Model 4, AIC: 92.569, a-value= 2.8; b-value: 0.846, weight: 0.24

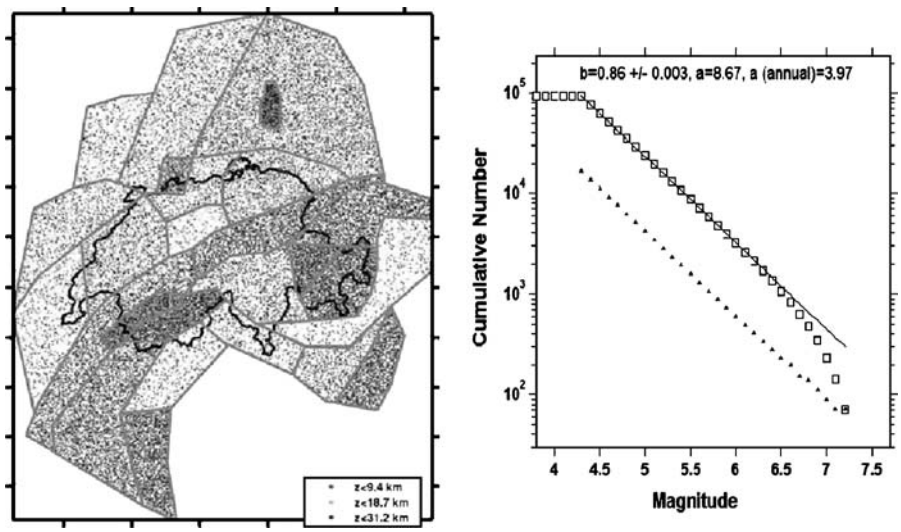

Fig. 8 Example of a synthetic catalog. *Left*: Map of epicenters and sources zones used in model SEIS. *Right*: Cumulative (*squares*) and non-cumulative (*triangles*) frequency–magnitude distribution of events. In this case, M_{max} was assumed 7.2. Note that for plotting purposes, the catalog in this figure contains only 50,000 years, and the map only displays events with $M \geq 5$

- M_{max} should not vary between zones; the choice of M_{max} is, in our opinion, a generic one. This reflects the assumption that no fundamental differences between tectonic regions exist in the study regions that would justify a different behavior when it comes to M_{max}.

To incorporate this principles, and to keep a simple model, we use only two different M_{max} as logic tree branches: M_{max} = 7.2 and M_{max} = 7.5. This model has the advantage of being simple, yet allowing capturing the influence of M_{max} for sensitivity analysis. As it will turn out, the hazard sensitivity to M_{max} is, as expected, only minor.

2.4 Predictive ground motion models

Ground motion relations, estimating ground motions as a function of earthquake magnitude and distance, are critical to seismic hazard assessment. A PGMM describes the attenuation of amplitude with distance due to geometrical spreading and intrinsic attenuation, as well as the scaling of amplitude with magnitude. The PGMM is generally the element with the largest influence on the final hazard results. It also is generally the largest contributor to uncertainties in hazard.

Numerous PGMMs have been proposed worldwide and specifically for central Europe in the last two decades (Douglas 2003). Most studies adopt a functional form introduced by Joyner and Boore (1981), with a constant geometrical spreading for all distances [e.g., Sabetta and Pugliese (1987) (Italy); Ambraseys et al. (1996) (Europe); Smit 1996 (Switzerland); Ambraseys et al. (2005) (Europe and Middle East)]. A different approach, applied by Malagnini et al. (2000a, b) in Italy and Germany, Malagnini and Herrmann (2000) in Italy, Morasca et al. (2006) in the Western Alp, and Malagnini et al. (2007) in the San Francisco Bay area, uses a stochastic simulation method (Boore 1983, 2003; Raoof et al. 1999) to predict ground motions.

Recently, a dedicated study of attenuation and scaling for Switzerland was published by Bay (2002) and Bay et al. (2003, 2005). Following the approach by Malagnini et al. (2000a, b) and Malagnini and Herrmann (2000), Bay et al. modeled spectral ground motion (1 to 15 Hz) as a function of distance for events spanning the magnitude range $3.0 < M_w \leq 7.0$ in Switzerland. The parameters were inverted from 2,958 horizontal and vertical component waveforms of small to moderate size events ($2.0 \leq M_L \leq 5.2$) in the distance range 10–300 km recorded on hard rock sites with an estimated shear-wave velocity

of about 1,500 m/s in the upper 30 m. The units are response-spectral displacements, pseudo-spectral velocities, and pseudo-spectral accelerations (Boore 2001, 2003). We use this study as the baseline for our PSHA of Switzerland.

The distinction between aleatory variability and epistemic uncertainty is now widely viewed as a useful paradigm for seismic hazard analysis (e.g., Toro et al. 1997). In PSHA, aleatory variability determines the shape of the hazard curve, whereas epistemic uncertainties, captured by the branches of the logic tree, lead to families of hazard curves (e.g., Bommer et al. 2005). Note, however, that while the distinction between aleatory and epistemic uncertainties is conceptually useful, in practice, the separation of the two is far from being clear cut.

We distinguish between the two parts of a ground motion model. (1) The true attenuation part, which we consider well described by the model given by Bay et al. (2003, 2005), because in our assumption, intrinsic attenuation and geometrical spreading are scale invariant. (2) The scaling with magnitude, on the other hand, may be poorly constrained based on the small to moderate events in Switzerland. Here, we use scaling relationships derived for other regions where large events have occurred.

Ground motion scaling is a currently much debated topic in seismology. It is critical when extrapolating towards larger magnitude events (Mayeda and Walter 1996; Ide and Beroza 2001; Ide et al. 2003). The critical scaling parameter often referred to is "stress drop", $\Delta\sigma$, or "apparent stress drop" (Brune 1970; Choy and Boatwright 1995), which is only somewhat related to the actual physical drop in stress during an earthquake (Atkinson and Beresnev 1997). Even in areas with excellent monitoring and with datasets containing several large events, such as California or Japan, it remains hotly debated if stress drop is constant or scales with magnitude. Bay et al. (2005) proposed a set of scaling models that are able to explain the small stress drop ($\Delta\sigma \approx 3$ bars) observed for M3 class events in Switzerland, but is consistent with observed damages from larger events and with worldwide scaling relationships. We use three different scaling models as input for the hazard computations in order to express epistemic uncertainty:

1. Increasing stress drop to a maximum of $\Delta\sigma \approx 30$ bars. In this model, which best fits the Swiss data at small magnitudes, stress drop scales proportionally to moment as $M_o^{0.25}$ as proposed by Mayeda and Walter (1996). The upper bound for this increase is set to a stress drop of $\Delta\sigma \approx 30$ bars, as it is found from a compilation of worldwide studies (Ide and Beroza 2001).
2. Same as model 1, but increasing to a maximum value of $\Delta\sigma \approx 50$ bars. This model assumes that the largest events may have a higher than average stress drop.
3. Constant stress drop of $\Delta\sigma \approx 30$ bars for all magnitudes. This model does not fit small magnitude seismicity in Switzerland well; however, it is a viable alternative for the hazard relevant event with $M \geq 5.0$ where no Swiss data is available.

We also considered using alternative European attenuation functions, such as the frequently used Ambraseys et al. (1996). The comparison between these PGMM (Bay et al. 2005) shows that for most distances, Ambraseys PGMM shows significantly higher ground motions; however, for distances of less than about 10 km, the Swiss models exhibit higher ground motions. While we are aware that comparing PGMM derived for different magnitude ranges is problematic (Bommer et al. 2007), we feel that it would not be appropriate to use Ambraseys PGMM or other European attenuation relationships because of the following reasons:

1. The site class of Ambraseys is different; his reference rock has a shear-wave velocity in the upper 30 m that is about half of the one estimated for our sites. While a conversion to a reference site is possible, this adds additional aleatory uncertainty and hence artificially increases the hazard (Scherbaum et al. 2005).
2. The magnitude scales are different. While Ambraseys M_S measurements can be converted to M_w, this again adds aleatory uncertainty and is difficult for magnitudes below

5.0 where M_S is not well defined. Such small events contribute significantly to the hazard in countries of moderate seismicity, as illustrated by the Dec. 8, 2006 M_w = 3.2 induced event underneath Basel that caused significant non-structural damage in Basel. We also feel that using a PGMM model that is derived based on the same magnitudes and site conditions used for recurrence estimation is most appropriate because this model is internally consistent.

3. The events considered and the tectonic environments are quite different. The majority of Ambraseys earthquakes stem from the Mediterranean area. Attenuation is different in Switzerland (Bay et al. 2003). Ambraseys PGMM does not well fit the Swiss data in terms of attenuation or scaling of small events.

The most appropriate choice of the PGMM model, however, remains a hotly debated issue in regions of low seismicity where one is forced to either extrapolate to larger magnitudes from the small ones, or "import" data from other regions. The attention experts of the PEGASOS group, for example, reached quite different conclusions on this issue (see for example Scherbaum et al. 2006).

2.4.1 Aleatory uncertainty of PGMM

Including aleatory uncertainty is critical (Bommer et al. 2005; Bommer and Abrahamson 2006). The aleatory uncertainty of the PGMM of Bay et al. (2005) includes parametric and modeling uncertainties. Bay et al. (2005) computed an average $\log_{10} \sigma_{lg} = 0.35$. Note, however, that this value includes scatter from source, path, and site effects. We feel that we are not able to divide σ_{lg} into intra- and inter-event contributions or reduce the site contamination because the available database is too sparse. When computing site-specific hazard, one has to be careful to consider that σ_{lg} already contains a sizeable (but unknown) site uncertainty component. We also—somewhat arbitrarily—truncate the uncertainty distribution of the PGMM at $2\sigma_{lg}$. While this truncation can influence the final hazard (Strasser et al. 2008), we will find in the subsequent sensitivity analysis shows that this truncation has little impact on the median or mean hazard results; however, it would becomes relevant for very low probability scenarios.

A final decision regarding the PGMM involves the shape of the model for very small distances. The PGMM cannot continue to increase proportionally to $1/r$ because the associated ground motion would approach infinity. No data are available for Switzerland to constrain this roll over distance, r_{min}, and very little data exist with hypocentral distances below 2 km worldwide. Because r_{min} is uncertain, we considered treating it as such through a logic tree branch, which allows us to also study the sensitivity of the results to this parameter. In our final model, we only use r_{min} = 1 km, since sensitivity analyses showed only a minor influence of r_{min} on hazard for the return periods we considered.

3 Hazard computation and results

3.1 Monte-Carlo simulation approach

Various computer codes to estimate seismic hazard based on a Cornell/McGuire-type approach are available, some commercial, some open source (Bender and Perkins 1987; Field et al. 2005). We decided to develop a synthetic catalog-based implementation of the Cornell–McGuire method to compute probabilistic seismic hazard for Switzerland and its uncertainty. Our method is, in principle, identical to Musson (2000). See also Beauval et al. (2006) for a review of the advantages of Monte Carlo-based hazard assessment in regions of distributed seismicity. Our code was validated against outputs of Frisk88 (Risk Engineering Inc.) for selected input models, which gave identical hazard curves for the same set of simple input models.

The process of hazard computation for a given frequency, including the logic tree branching shown in Figs. 8 and 9, follows these four steps:

1. Create a synthetic catalog of earthquakes for one logic tree branch based on the zoning model as well as on M_c, a and b, and M_{max} parameters in each source zone. The catalog spans one million years and contains events down

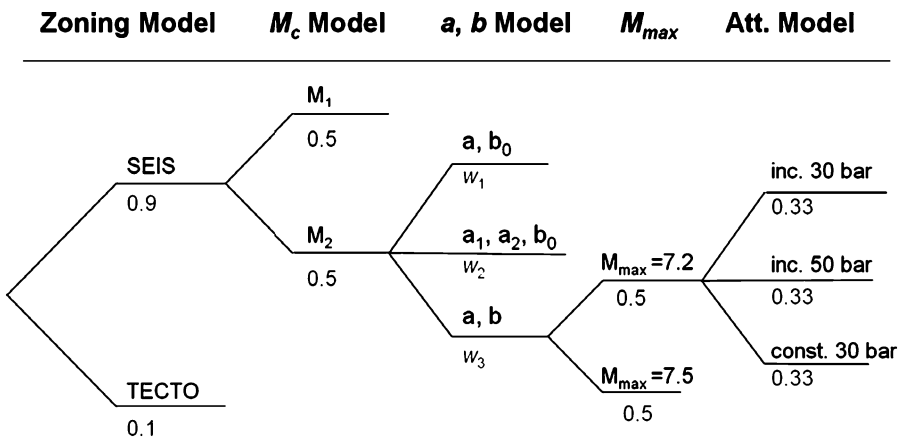

Fig. 9 Logic tree setup of the hazard model. Weights for each branch are given in *gray beneath the branch*. For the *a* and *b* value estimation, the weight (w) is zone-dependent

to magnitude 4.0, typically two million events. The depths of events are explicitly given.

2. Alternative source zonations, completeness, a, b, and $M_{\max}$ models result in alternative catalogs, a total of 24 in our case ($2 \times 2 \times 3 \times 2 = 24$ branches). The three alternative a and b models and their weighting are considered within each catalog by creating subcatalogs of a duration that corresponds to the AIC_c weighting factor (e.g., weight 0.6 = 600,000 years). One example of such a catalog and its frequency–magnitude distribution is shown in Fig. 8.
3. Three alternative predictive ground motion models at a given frequency f_i result in three branches.
4. Each earthquake E_i from the catalog creates a ground motion Y_i at the receiver site R_i, computed based on the PGMM and a randomly drawn uncertainty in the range of $\pm 2\sigma_{\lg}$. We rank these ground motions in descending order starting with the highest observed ground motion in any 1-year period. From these, we can extract the annual probability of exceedance for any given probability level (Musson 2000).

The total number of alternative branches considered is 72. We compute the median hazard and any desired fractiles, for example the 16 and 84 percentiles that represent the one-sigma standard deviation. We choose the median hazard curve following the arguments spelled out by Abrahamson and Bommer (2005). To compute hazard maps, this procedure is repeated for all nodes spaced evenly on a 5 × 5-km grid covering Switzerland.

3.2 Hazard results

We present selected results only; the complete PSHA results for a range of frequencies and return periods, including also uniform hazard spectra, are available on the SED web page, www.seismo.ethz.ch. We compute and show only accelerations in units of 5% damped acceleration response spectrum at a given frequency. Velocities or displacements could also be computed using the PGMM of Bay et al. (2005). First of all, we plot seismic hazard curves (annual probability of exceedance as a function of spectral acceleration) for four selected sites in Switzerland, the locations of Basel, Sion, Zurich, and Bern (Fig. 10). As expected, results show the highest hazard at Sion in the Wallis where historically (Fig. 2), most of the damaging events have been located. A seismic hazard map, in units of 5% damped acceleration response spectrum (in cm/s^2 at 5 Hz frequency), is shown in Fig. 11. The maximum acceleration observed at 5 Hz is 151 cm/s^2, respectively, and located in the Wallis. Other areas of increased hazard are located in the Basel region, along the Helvetic Front and in Graubünden. The maps are calibrated for a rock ground condition (a shear wave velocity of approximately 1,500 m/s in the upper 30 m). For softer soil conditions, site amplifications must be considered and can be on the order of a factor of 2–4 with respect to hard rock conditions (Fäh et al. 2003). We also plot the hazard maps for 1-Hz frequency for return periods

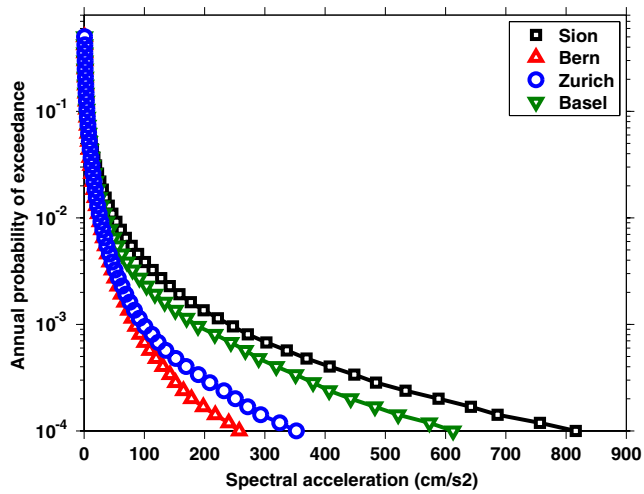

Fig. 10 Hazard curves for four cities in Switzerland. Plotted is the median annual probability of exceedance as a function of ground acceleration in units of 5% damped acceleration response spectrum at 5 Hz

of 100, 475, 2,500, and 10,000 years in Fig. 12. Their values of course are much lower than the ones for higher frequencies. In addition, one notices that the hazard is slightly less concentrated, which is a result of the reduced slope of the attenuation function at lower frequencies (Bay et al. 2003).

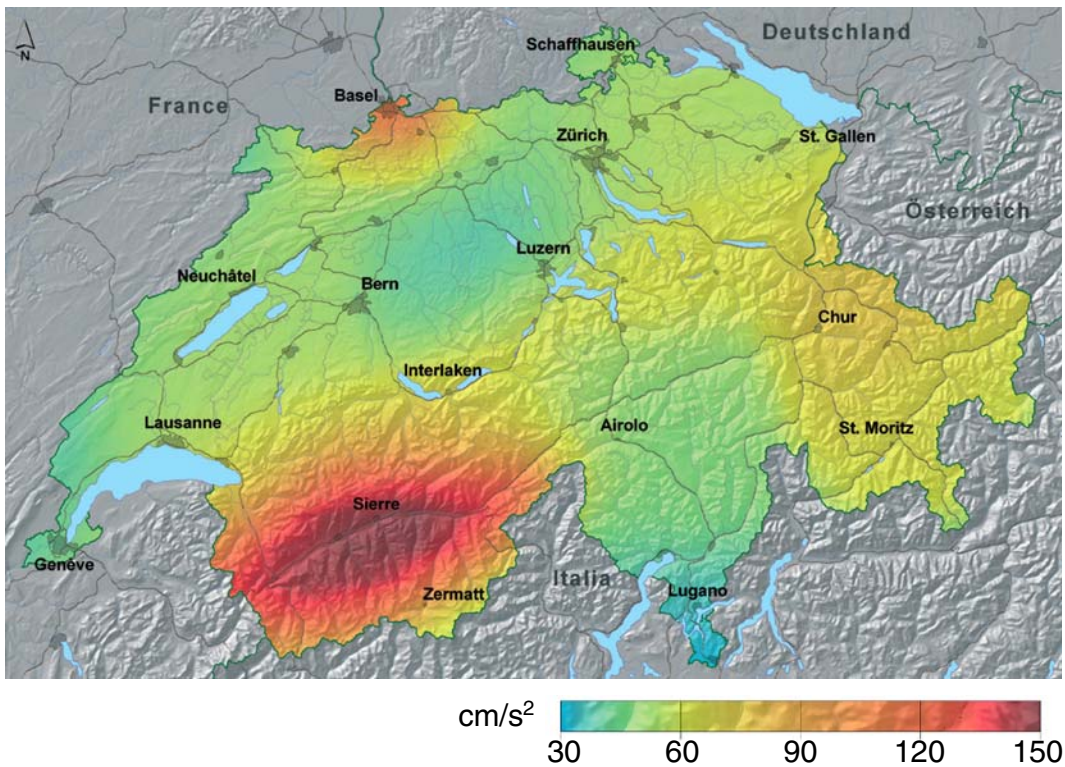

Fig. 11 Seismic hazard map of Switzerland depicting the level of horizontal ground motion in cm/s^2 (in units of 5% damped acceleration response spectrum at 5-Hz frequency) expected to be reached or exceeded in a period of 475 years (10% exceedance chance in 50 years). The map is calibrated for a rock ground condition (V_s approximately 1,500 m/s). Overall, the hazard level of Switzerland ranges between 5% and 15% of the acceleration of gravity (50–150 cm/s^2)

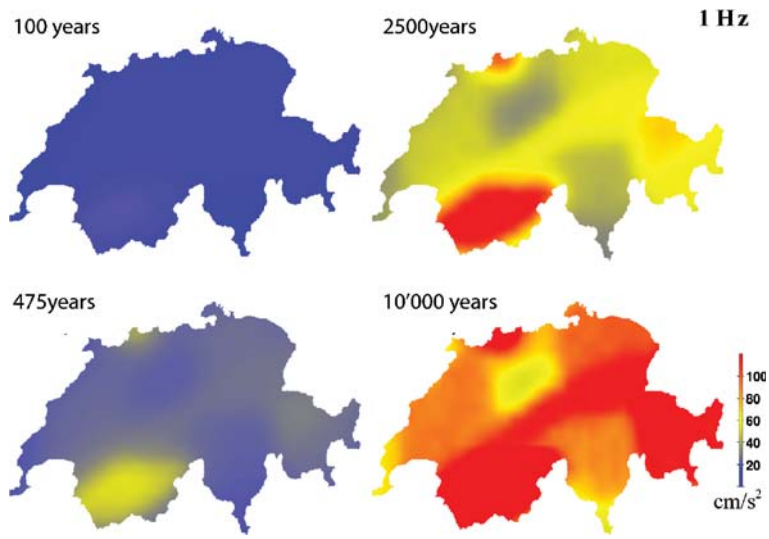

Fig. 12 Same as Fig. 11, but for return periods of 100, 475, 2,500, and 10,000 years and a 1-Hz frequency. Note that the scale (cm/s^2) for the longest return period is clipped in order to use just one scale

With longer return periods, hazard is more concentrated in the areas of highest hazard, the Wallis and Basel. In other words, the difference between the lowest hazard areas in Switzerland, the Ticino, and the highest hazard area, the Wallis, increases from about a factor of 2 for return periods of 100 years to a factor of 7 for return periods of 10,000 years. This is a result of the lower b values in the high hazard areas in some models, which become increasingly relevant for longer return periods.

3.3 De-aggregation of hazard results

De-aggregation of hazard is required to understand what types of events contribute most to the hazard for a given site. After specifying for a given frequency a return period, one then determines from which magnitude and distance range the hazard to a site stems. The results of the de-aggregation depend on the site of interest. We show for example results from one site only (Sion, Fig. 13). The general trend of all de-aggregation results is that for longer recurrence intervals, the main hazard contribution comes from larger events and closer-by distances. The overall shape of the de-aggregation plots is determined by the attenuation relation, while the spread of the values is largely a result of the sigma of the attenuation relation.

For Sion, we find that for a recurrence period of 100 years (spectral acceleration 53 cm/s^2), most hazard is contributed from magnitude 4–5 events at distances of 5–15 km (black squares in Fig. 13). Note, however, that such small earthquakes produce high peak accelerations at short distances, but their potential for widespread damage is limited because of their short duration and low energy content. Larger distances and magnitudes also contribute (gray squares). For 475 years (spectral acceleration 151 cm/s^2), magnitude 5.0–6.0 events dominate. At 2,500 and 10,000 years (spectral accelerations of 368 and 708 cm/s^2, respectively), we find that most hazard is still contributed from magnitude 5.0–6.5 events at distances of 5–10 km. However, even at these large ground motion levels, events of M5 or smaller contribute significantly to the hazard; these events would be very close to the site and thus cause unusually large ground motions.

For other sites, such as Basel and Zurich (not shown), the results are quite comparable. A larger contribution to the hazard comes from deeper events, which is a result of the greater hypocentral depths in the Foreland compared to the Alps. For return periods of 2,500 and 10,000 years, for Basel, we find a larger contribution from the higher magnitude range, similar to Sion. It is interesting to note that even for long return periods, the rare largest events ($M \geq 7$) are not a significant contributor to design hazard.

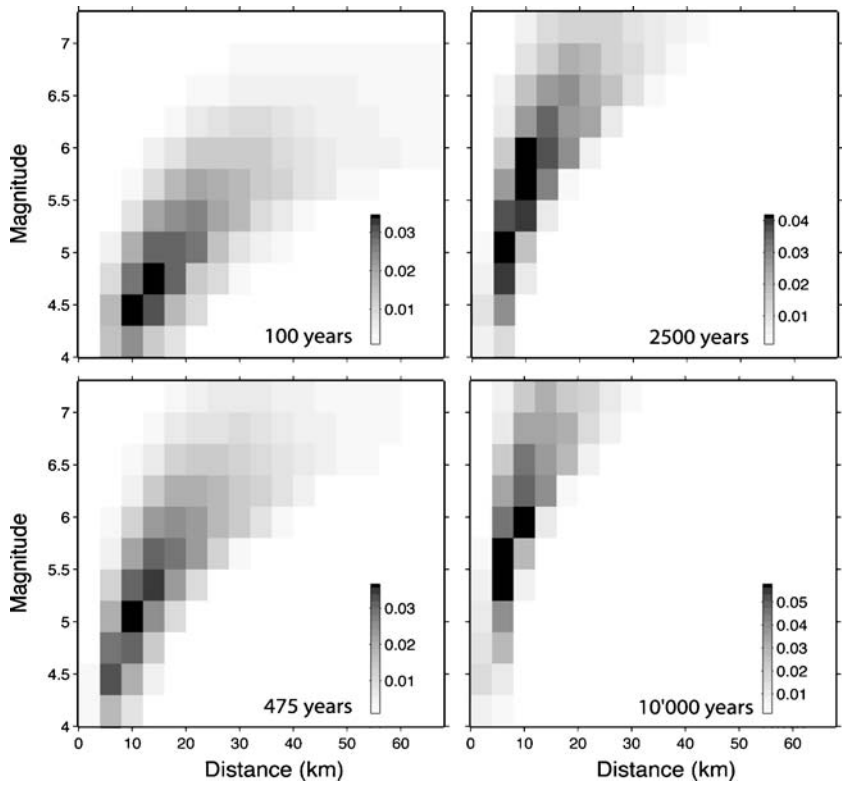

Fig. 13 De-aggregation of the hazard results (in units of 5% damped acceleration response spectrum at 5-Hz frequency) for the site of Sion. The *grayscale* shows the fractional contribution of each magnitude–distance bin. The different frames shows four return periods: 100, 475, 2,500, and 10,000 years

3.4 Sensitivity to input parameters

Sensitivity is studied in order to detect which parameters are the most critical for the hazard computation. This can also offer guidance for future research activities. A number of input decisions were made based on sensitivity feedback computed from a preliminary hazard model. This helped us to determine that:

- The type of declustering does not play a significant role in the hazard assessment; Reasenberg (1985) declustering or the (Gardner and Knopoff 1974) approach with different sets of input parameters do not significantly change the hazard output. Therefore, we decided to not include a logic tree alternative branch for different declustering algorithms.
- Similarly, removing explosion events does not play a significant role; hazard results do not change significantly if dequarrying is applied or not. Therefore, no logic tree alternative branch is included for different dequarring.
- Soft borders in the hazard computation (gradually changing rates across zone boundaries) do not play a significant role as long as the smoothing distance remains small. Therefore, again, no logic tree alternative branch is included for different border types.
- The choice of the magnitude of completeness (M_c) model has a moderate influence on the final hazard, M_c model 2 results show up to 10% higher values overall, and, specifically for the Wallis region, with a slightly different spatial distribution of hazard.

In Fig. 14, we show sensitivity analysis for eight parameters, all computed for 5 Hz and a site in the

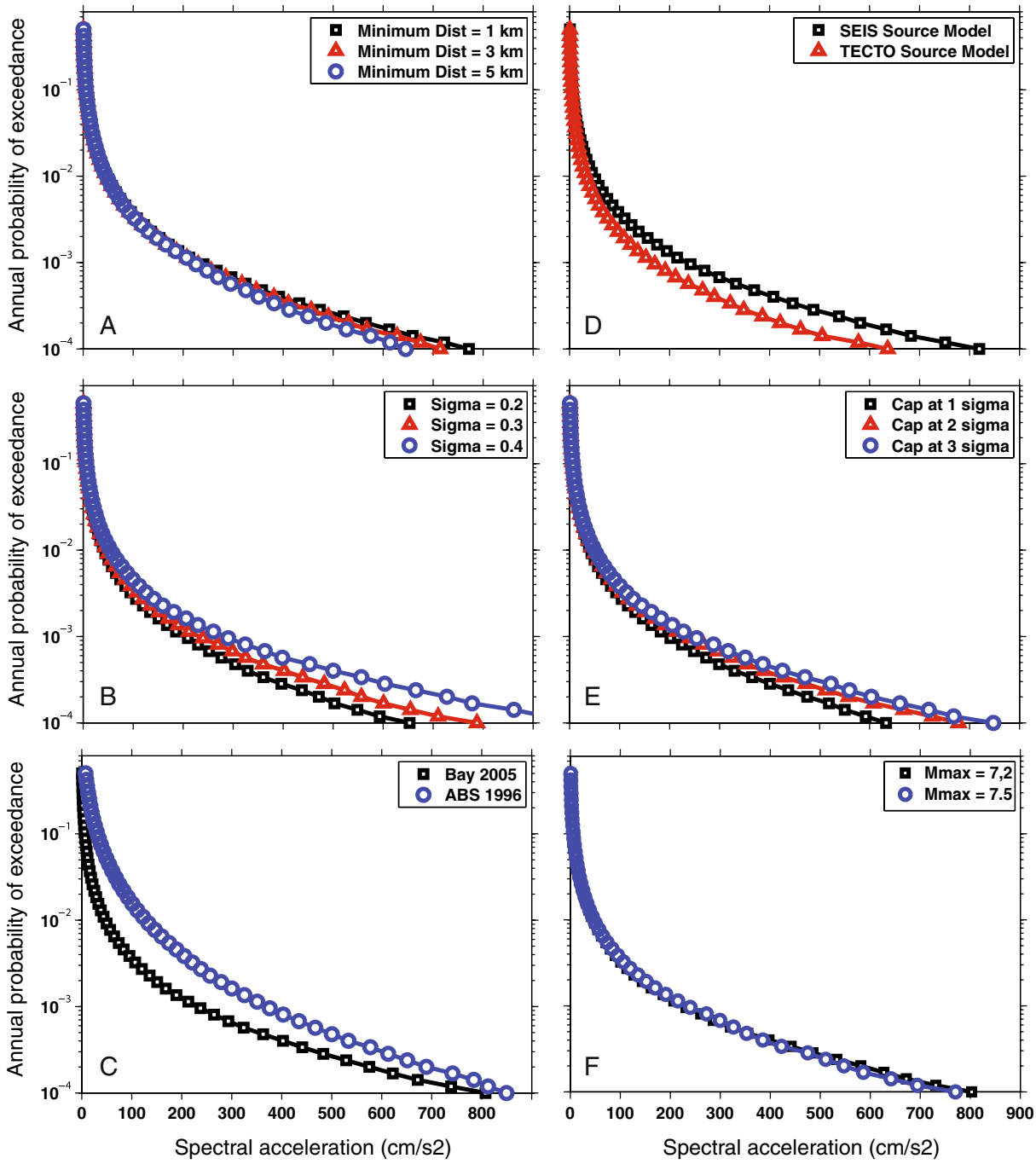

Fig. 14 Sensitivity analysis. Plotted are hazard curves (annual probability of exceedance as a function of ground acceleration in units of 5% damped acceleration response spectrum at 5 Hz) for a site in the Wallis (Martigny), each evaluating the sensitivity to a specific input parameter of the hazard model: **a** Minimum distance of the PGMM; **b** Sigma of the PGMM; **c** Comparison between the Ambraseys et al. (1996) and Bay et al. (2005) attenuation laws; **d** SEIS and TECTO source models; **e** Cap of the sigma in the attenuation law; **f** Maximum magnitude

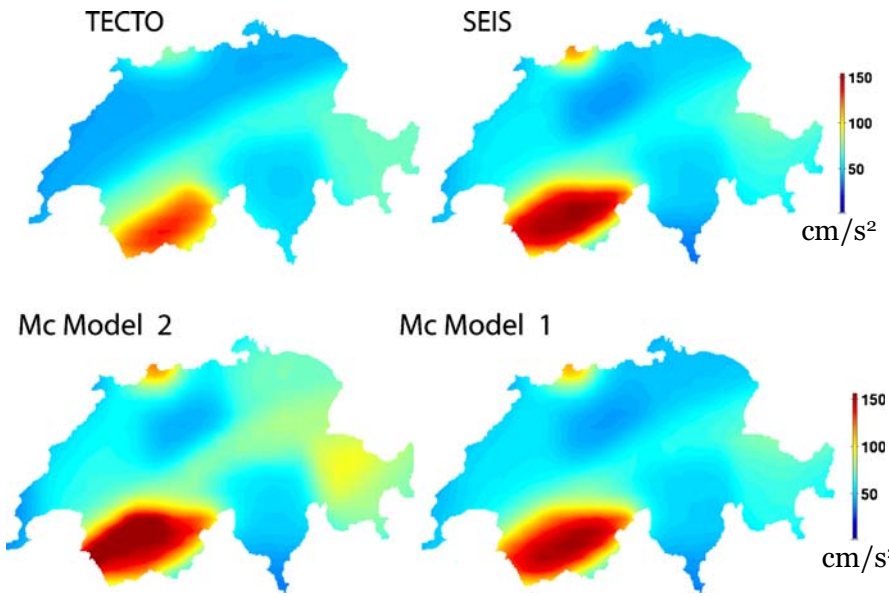

Fig. 15 *Top frames* Hazard maps at 5 Hz/475-year return period (spectral acceleration in cm/s^2) for the two different zoning approaches. *Left*: Model TECTO. *Right*: Model SEIS. *Bottom frames*: Hazard maps at 5 Hz/475-year return period (spectral acceleration in cm/s^2) compared are the different completeness models

Wallis (Martigni). From these figures, we derive that minimum distance used in the PGMM (Fig. 14a) has a minimal effect only on the hazard curve. The sigma of the attenuation (Fig. 14b) influences the hazard curve quite strongly, especially at low annual probabilities of exceedance. This is consistent with other hazard studies (e.g., Bommer and Abrahamson 2006) and suggest also that a critical step in improving the hazard assessment is related to an improved understanding of the scatter of ground motions. In Fig. 14c, we compare the hazard curves computed based on the Bay et al. (2005) PGGM model employed in this study with the one computed based on the Ambraseys et al. (1996) attenuation. The difference between the two PGMM is largest for intermediate annual probability of exceedance, with Bay et al. (2005) being up to one third lower. This is explained by the fact that the contribution to the hazard at intermediate probabilities is dominated by events in the range 4.5–5.5 where the difference between the two PGMM is largest (Bay et al. 2005). The choice of the zoning model has a moderate impact on the resulting hazard (Fig. 14d), with the SEIS model resulting in hazard of up to 20% higher than TECTO at long return periods. The sensitivity analysis of the truncation level of the PGMM (Fig. 14e) suggests that the difference of a cut at 2 or 3 sigma is minimal. Lastly, the choice of the maximum magnitude $M_{\max}$ has a minor influence on the hazard (Fig. 14f).

When comparing the hazard maps at 5 Hz for a return period of 475 years for the SEIS and TECTO models (Fig. 15), we find that the latter reaches peak values about 25% lower than the first. The overall appearance of the TECTO model is smoother; a result of the larger source zones (Fig. 4). Specifically, the hazard at Basel is reduced in absolute terms and relative to other regions, such as Graubünden.

4 Conclusions

In this study, we present and discuss the new generation of probabilistic seismic hazard assessment for Switzerland. This study replaces the previous intensity-based generation of national hazard maps of 1978.The PSHA builds upon extensive research and database compilation over the last 10 years. Progress was made in particular by using a Swiss specific PGMM, which provides physical units of acceleration, velocity, or displacement. In addition, both the historical and instrumental earthquake database were vastly improved and converted to a uniform moment magnitude scale. We also developed a new zonation, which takes into account an improved understanding of the

seismotectonic framework of the region. Finally, we implemented a 72-branch logic tree to characterize uncertainty in the seismic hazard. The final model, the new national seismic hazard assessment for Switzerland, was released in late 2004. The new national building code of Switzerland (SIA code 261 2003) already reflects the changes seen in the 2004 hazard model both in terms of the zoning of Switzerland as well as the design acceleration. While the full PSHA was not ready at the time that the SIA code was designed, a preliminary version was available.

The presented hazard model differs from previous assessments in a few aspects. It is not possible to compare absolute values, since the old generation of hazard assessment was created from an intensity-based attenuation relation. While the main activity centers in the Wallis and Basel remain dominant in the hazard, the hazard maps presented here (Fig. 11) are smoother across the country. Smoother hazard is found specifically along the Alpine Front, in the Graubünden, and in the Wallis. These changes reflect the realization of seismologists that the instrumental and historical record is too short to be simply extrapolated into the future. Events of magnitude 6–7 are now believed to be possible in all regions of Switzerland, but in areas of low seismicity, their recurrence intervals may be too long (>10,000 years) to be known from the historical or even the paleoseismic record.

The fact that temporal and spatial nonstationarity of the earthquake catalog today is clearly seen but not easily understood. We do not know why regions such as the Wallis are periodically more active for some years to decades, and we have currently no means of forecasting the next periods of higher activity. The Wallis, for example, has been relatively quiet in the past 30 years when compared to other periods of history—but what does that imply for the next 30 years? Consequently, current PSHA for Switzerland must assume a time-independent Poissonian recurrence model, which results in larger uncertainties. Likewise, the physical processes that determine spatial and temporal changes in the earthquake size distribution are poorly understood and hence cannot be integrated well into a predictive model other than by extrapolation of the past. While we have made some progress in understanding spatial variability in b values (e.g., Schorlemmer et al. 2004a, b), there remains a significant research need.

PSHA inevitably involves a certain level of expert opinion in the decision-making process and also the logic tree branch weighting needed for the final model because our knowledge of the underlying processes is incomplete. The model and its input parameters were reviewed by a team of experts from within the SED; however, a different group of experts would make somewhat different decisions. The group of PEGASOS experts, for example, has derived an extensive set of zoning model for the site-specific hazard assessment of the three sites of nuclear power plants in Switzerland (Klügel 2005, 2007). We are not in a position to quantitatively compare the very complex PEGASOS zoning and recurrence models to the much more simple ones derived here; however, because both rely on the ECOS earthquake catalog, we speculate that the difference are comparatively small. With respect to the PGMM, however, differences between the PEGASOS experts and our assessment are significant: The PGMM we use, based on Bay et al. (2005), results in significantly lower hazard when compared to other PGMM (e.g., Fig. 14c, also Scherbaum et al. 2006). Because our PGMM is consistent with the SED M_w magnitude scale and site conditions in Switzerland, thus reducing the need for additional conversions because it is consistent with the observed ground motions of small events and calibrated in its stress drop to global observations, we feel that the decision made for the Swiss National Seismic Hazard model is sensible. The PEGASOS PGMM results are currently being reviewed in a follow-up project, and an update of Bay et al. (2005) including more digital broadband waveform data collected in the past few years is also on the way, hopefully allowing to resolve the difference between the models.

Our hazard model, while largely following the well-established route of PSHA established by Cornell (1968) and McGuire (1976), includes several innovative aspects. Most importantly, we introduce a more objective way to assess the b values in individual zones. Using the AIC_c, we

are able to decide, based on an established statistical criterion, if the data in a specific zone warrants to be fitted with a zone specific b value or if the overall b value is superior. Using AIC weights, we are able to express objectively a range of alternative scenarios for the different (a, b) models. This addresses a long-standing need in hazard assessment, and it stabilizes the resulting model by avoiding large fluctuations in b values. We recommend using such procedures in future hazard assessments as a tool to improve the model generation.

The new PSHA presented here is the culmination point of many years of investigations by a diverse group of researchers. However, the progress in our understanding of the earthquake process, as well as the collection of new data and the development of innovative approaches, is not stopping. The SED is working toward the future generation of seismic hazard for Switzerland, anticipated for around the year 2011.

Acknowledgements The authors are indebted to all who contributed in small or large part to the assessment of the seismic hazard of Switzerland. Special thanks to the M. Baer, F. Bay, A. Becker, F. Bernardi, J. Braunmiller, M. Ferry, S. Jenny, M. Garcia-Jiménez, M. Gisler, S. Heimers, S. Husen, P. Kästli, U. Kastrup, F. Kind, U. Kradolfer, M. Mai, S. Maraini, K. Monecke, M. Schnellmann, D. Schorlemmer, G. Schwarz-Zanetti, S. Steimen, J. Wössner, S. Wöhlbier and A. Wyss. This work was supported by ETHZ, the Swiss Nuclear Safety Board (HSK), the Swiss National Foundation (SNF), Swissnuclear and by reinsurance and insurance broker companies (SwissRe, MünichRe, Benfield Greig). We like to thank J Bommer, one anonymous reviewers and the associate editor, G. Grünthal, for their detailed input that greatly helped to improve the manuscript.

References

Abrahamson NA, Bommer JJ (2005) Probability and uncertainty in seismic hazard analysis. Earthq Spectra 21(2):603–607. doi:10.1193/1.1899158

Abrahamson NA, Birkhauser P, Koller M, Mayer-Rosa D, Smit PM, Sprecher C et al (2002) PEGASOS—a comprehensive probabilistic seismic hazard assessment for nuclear power plants in Switzerland. In: Proceedings of the 12 ECEE, London, paper no. 633

Akaike H (1974) New look at statistical-model identification. IEEE Trans Automat Contr AC19(6):716–723. doi:10.1109/TAC.1974.1100705

Aki K (1965) Maximum likelihood estimate of b in the formula log N = a – b M and its confidence limits. Bull Earthq Res Inst 43:237–239

Ambraseys N (2003) Reappraisal of magnitude of 20th century earthquakes in Switzerland. J Earthq Eng 7: 149–191. doi:10.1142/S1363246903001073

Ambraseys NN, Simpson KA, Bommer JJ (1996) Prediction of horizontal response spectra in Europe. Earthq Eng Struct Dyn 25:371–400. doi:10.1002/(SICI)1096-9845(199604)25:4<371::AID-EQE550>3.0.CO;2-A

Ambraseys NN, Douglas J, Sarma SK, Smit PM (2005) Equations for the estimation of strong ground motions from shallow crustal earthquakes using data from Europe and the Middle East: horizontal peak ground acceleration and spectral acceleration. Bull Earthq Eng 3:1–53. doi:10.1007/s10518-005-0-0183-0

Atkinson GM, Beresnev I (1997) Don't call it stress drop. Seismol Res Lett 68:3–4

Bakun WH, Wentworth CM (1999) Estimating earthquake location and magnitude from seismic intensity data (vol 87, p 1502, 1997). Bull Seismol Soc Am 89(2): 557–557

Bay F (2002) Ground-motion scaling in Switzerland: implications for hazard assessment. PhD thesis no. 14567, Swiss Federal Institute of Technology, Zurich

Bay F, Fäh D, Malagnini D, Giardini D (2003) Spectral shear wave ground-motion scaling in Switzerland. Bull Seismol Soc Am 93:414–429. doi:10.1785/0120010232

Bay F, Wiemer S, Fäh D, Giardini D (2005) Predictive ground-motions relationships for Switzerland: best estimates and uncertainties. J Seismol 9:223–240. doi:10.1007/s10950-005-5129-0

Beauval C, Hainzl S, Scherbaum F (2006) The impact of the spatial uniform distribution of seismicity on probabilistic seismic-hazard estimation. Bull Seismol Soc Am 96:2465–2471. doi:10.1785/0120060073

Becker A, Davenport CA (2003) Rockfalls triggered by the A.D. 1356 Basle earthquake. Terra Nova 15(4):258–264. doi:10.1046/j.1365-3121.2003.00496.x

Becker A, Davenport CA, Giardini D (2002) Palaeoseismicity studies on end-Pleistocene and Holocene lake deposits around Basle, Switzerland. Geophys J Int 149(3):659–678. doi:10.1046/j.1365-246X.2002.01678.x

Bender B (1983) Maximum likelihood estimation of b-values for magnitude grouped data. Bull Seismol Soc Am 73:831–851

Bender B, Perkins DM (1987) SEISRISK III: a computer program for seismic hazard estimation. US Geol Surv Bull 1772:20

Bommer JJ, Abrahamson NA (2006) Why do modem probabilistic seismic-hazard analyses often lead to increased hazard estimates? Bull Seismol Soc Am 96:1967–1977. doi:10.1785/0120060043

Bommer JJ, Abrahamson NA, Strasser FO et al (2004) The challenge of defining upper bounds on earthquake ground motions. Seismol Res Lett 75(1):82–95

Bommer JJ, Scherbaum F, Bungum H et al (2005) On the use of logic trees for ground-motion prediction equa-

tions in seismic-hazard analysis. Bull Seismol Soc Am 95(2):377–389. doi:10.1785/0120040073
Bommer JJ, Stafford PJ, Alarcón JE, Akkar S (2007) The influence of magnitude range on empirical ground-motion prediction. Bull Seismol Soc Am 97(6): 2152–2170. doi:10.1785/0120070081
Boore DM (1983) Stochastic simulation of high-frequency ground-motion based on seismological models of the radiated spectra. Bull Seismol Soc Am 73:1865–1894
Boore DM (2001) Fortran programs for simulating ground-motions from earthquakes: version 2.0—a revision of Open-File Report 96-80-A. Open-File Report 00-509, US Geological Survey
Boore DM (2003) Prediction of ground-motion using the stochastic method. Pure Appl Geophys 160:635–676. doi:10.1007/PL00012553
Boore DM et al (1997) Equations for estimating horizontal response spectra and peak acceleration from western North America earthquakes: a summary of recent work. Seism Res Lett 68:128–153
Braunmiller J, Deichmann N, Giardini D, Wiemer S (2005) Homogeneous moment magnitude calibration in Switzerland. Bull Seismol Soc Am 95(1):58–74
Brune JN (1970) Tectonic stress and the spectra of seismic shear waves from earthquakes. J Geophys Res 75:4997–5009. doi:10.1029/JB075i026p04997
Budnitz RJ, Apostolakis A, Boore DM et al (1997) Recommendations for PSHA: guidance on uncertainty and use of experts (No. NUREG/CR-6372-V1)
Burg JP, Van Den Driessche J, Brun JP (1994) Syn- to post-thickening extension in the Variscan Belt of Western Europe: mode and structural consequences. Géol Fr 3:33–51
Burkhard M (1990) Aspects of the large-scale Miocene deformation in the most external part of the Swiss Alps (Subalpine Molasse to Jura fold belt). Eclogae Geol Helv 83(3):559–583
Choy GL, Boatwright J (1995) Global patterns of radiated seismic energy and apparent stress. J Geophys Res 100:18205–18226. doi:10.1029/95JB01969
Coppersmith KJ (1994) Conclusions regarding maximum earthquake assessment. The earthquakes of stable continental regions, 1: assessment of large earthquake potential. Electric Power Research Institute, Report TR-102261-V1, 1: a, 6-1-6-24
Cornell CA (1968) Engineering seismic risk analysis. Bull Seismol Soc Am 58:1583–1606
Cotton F, Scherbaum F, Bommer JJ, Bungum H (2006) Criteria for selecting and adjusting ground-motion models for specific target regions: application to Central Europe and rock sites. J Seismol 10(2):137–156. doi:10.1007/s10950-005-9006-7
Deichmann N (1992) Structural and rheological implications of lower-crustal earthquakes below northern Switzerland. Phys Earth Planet Inter 69:270–280. doi:10.1016/0031-9201(92)90146-M
Deichmann N, Baer M, Braunmiller J et al (2000) Earthquakes in Switzerland and surrounding regions during 1999. Grunthal 93:23–45
DeMets C, Gordon RG, Argus DF, Stein S (1990) Current plate motions. Geophys J Int 101:425–478. doi:10.1111/j.1365-246X.1990.tb06579.x
Douglas J (2003) Earthquake ground motion estimation using strong-motion records: a review of equations for the estimation of peak ground acceleration and response spectral ordinates. Earth Sci Rev 61(1–2):43–104. doi:10.1016/S0012-8252(02)00112-5
Eckardt P, Funk HP, Labhart T (1983) Postglaziale Krustenbewegungen an der Rhein-Rhone-Linie, Vermessung, Photogrammetrie. Kult Tech 2:43–56
Fäh D, Koch K (2002) Discrimination between earthquakes and, chemical explosions by multivariate statistical analysis: a case study for Switzerland. Bull Seismol Soc Am 92(5):1795–1805. doi:10.1785/012000166
Fäh D, Giardini D, Bay F et al (2003) Earthquake Catalogue Of Switzerland (ECOS) and the related macroseismic database. Eclogae Geol Helv 96(2):219–236
Field EH, Gupta N, Gupta V et al (2005) Hazard calculations for the WGCEP-2002 earthquake forecast using OpenSHA and distributed object technologies. Seismol Res Lett 76(2):161–167
Frankel A (1995) Mapping seismic hazard in the central and eastern United States. Seismol Res Lett 66:8–21
Frankel A, Harmsen S, Mueller C et al (1997a) U. S. G. S. national seismic hazard maps: uniform hazard spectra, de-aggregation, and uncertainty. In: Proceedings, FEMA/NCEER workshop on the national representation of seismic ground motion for new and existing bridges
Frankel A, Mueller C, Barnhard T et al (1997b) Seismic hazard maps for California, Nevada and western Arizona/Utah. United States Geological Survey Open-File Report, pp 97–130
Gardner JK, Knopoff L (1974) Is the sequence of earthquakes in Southern California, with aftershocks removed, Poissonian? Bull Seismol Soc Am 64: 1363–1367
Giardini D (1999) The global seismic hazard assessment program (GSHAP)—1992/1999. Ann Geofis 42: 957–974
Giardini D, Grünthal G, Shedlock KM, Zhang PZ (1999) The GSHAP global seismic hazard map. Ann Geofis 42(6):1225–1230
Grünthal G (1999) Seismic hazard assessment for Central, North and Northwest Europe: GSHAP region 3. Ann Geofis 42(6):999–1011
Grünthal G, Mayer-Rosa D, Lenhardt WA (1998) Abschätzung der Erdbebengefährdung für die D-A-CH-Staaten—Deutschland, Österreich, Schweiz. Bautechnik 10:753–767
Gutenberg R, Richter CF (1944) Frequency of earthquakes in California. Bull Seismol Soc Am 34:185–188
Hsü KJ (1995) The geology of Switzerland. Princeton University Press, Princeton, New Jersey, USA
Husen S, Kissling E, Deichmann N, Wiemer S, Giardini D, Baer M (2003) Probabilistic earthquake location in complex three-dimensional velocity models: application to Switzerland. J Geophys Res 108(B2):ESE5.1–ESE5.20. doi:10.1029/2002JB001778

Ide S, Beroza G (2001) Does apparent stress vary with earthquake size? Geophys Res Lett 28:3349–3352. doi:10.1029/2001GL013106

Ide S, Beroza GC, Prejean SJ, Ellsworth WL (2003) Apparent break in earthquake scaling due to path and site effects on deep borehole recordings. J Geophys Res 108(B5):2271. doi:10.1029/2001JB001617

Imoto M (1991) Changes in the magnitude frequency *b*-value prior to large (*M*-greater-than-or-equal-to-6.0) earthquakes in Japan. Tectonophysics 193(4):311–325. doi:10.1016/0040-1951(91)90340-X

Jaboyedoff M, Pastorelli S (2003) Perturbation of the heat flow by water circulation in a mountainous framework: examples from the Swiss Alps. Eclogae Geol Helv 96:37–47

Jiménez MJ, Giardini D, Grünthal G (2003) The ESC-SESAME unified hazard model for the European–Mediterranean region. EMSC/CSEM Newsletter 19: 2–4

Johnston AC, Coppersmith KJ, Kanter LR, Cornell CA (1994) The earthquakes of stable continental regions, vol. 1: assessment of large earthquake potential. Electric Power Research Institute (EPRI TR-102261-V1)

Joyner WB, Boore BM (1981) Peak horizontal acceleration and velocity from strong motion records including records from the 1979 Imperial Valley, California, earthquake. Bull Seismol Soc Am 71:2011–2083

Kagan Y (1999) Universality of the seismic moment–frequency relation. Pure Appl Geophys 155:537–574. doi:10.1007/s000240050277

Kagan Y, Jackson DD (2000) Probabilistic forecasting of earthquakes. Geophys J Int 143:438–453. doi:10.1046/j.1365-246X.2000.01267.x

Kastrup U (2002) Seismotectonics and stress field variations in Switzerland. PhD thesis no. 14527, ETH Zurich, 153 pp

Kastrup U, Zoback ML, Deichmann N, Evans K, Michael AJ, Giardini D (2004) Stress field variations in the Swiss Alps and the northern Alpine Foreland derived from inversion of fault plane solutions. J Geophys Res 109:B01402. doi:10.1029/2003JB002550

Kastrup U, Deichmann N, Frohlich A et al (2007) Evidence for an active fault below the northwestern Alpine foreland of Switzerland. Geophys J Int 169(3):1273–1288. doi:10.1111/j.1365-246X.2007.03413.x

Kenneth P, Burnham KP, Anderson DR (2002) Model selection and multimodel inference: a practical information—theoretic approach. Springer, New York

Kijko A, Graham G (1998) Parametric-historic procedure for probabilistic seismic hazard analysis - Part I: estimation of maximum regional magnitude m(max). Pageoph 152(3):413–442

Kijko A, Graham G (1999) "Parametric-historic" procedure for probabilistic seismic hazard analysis—part II: assessment of seismic hazard at specified site. Pure Appl Geophys 154(1):1–22. doi:10.1007/s000240050218

Kijko A, Lasocki S, Graham G (2001) Non-parametric seismic hazard in mines. Pure Appl Geophys 158 (9–10):1655–1675. doi:10.1007/PL00001238

Kissling E (1993) Deep-structure of the Alps—what do we really know. Phys Earth Planet Inter 79(1–2):87–112. doi:10.1016/0031-9201(93)90144-X

Klügel JU (2005) Problems in the application of the SSHAC probability method for assessing earthquake hazards at Swiss nuclear power plants. Eng Geol 78 (3–4):285–307. doi:10.1016/j.enggeo.2005.01.007

Klügel JU (2007) Error inflation in probabilistic seismic hazard analysis. Eng Geol 90(3–4):186–192. doi:10.1016/j.enggeo.2007.01.003

Knopoff L (1964) Statistics of earthquakes in California. Bull Seismol Soc Am 54:1871–1873

Koch K, Fäh D (2002) Identification of earthquakes and explosions using amplitude ratios: the Vogtland area revisited. Pure Appl Geophys 159(4):735–757. doi:10.1007/s00024-002-8657-3

Lomax A, Zollo A, Capuano P, Virieux J (2001) Precise, absolute earthquake location under Somma-Vesuvius volcano using a new three-dimensional velocity model. Geophys J Int 146(2):313–331. doi:10.1046/j.0956-540x.2001.01444.x

Malagnini L, Herrmann RB (2000) Ground-motion scaling in the region of the 1997 Umbria-Marche earthquakes (Italy). Bull Seismol Soc Am 90:1041–1051. doi:10.1785/0119990150

Malagnini L, Hermann L, Di Bona L (2000a) Ground-motion scaling in the Apennines (Italy). Bull Seismol Soc Am 90:1062–1081. doi:10.1785/0119990152

Malagnini L, RB Herrmann RB, Koch K (2000b) Regional ground-motion scaling in central Europe. Bull Seismol Soc Am 90:1052–1061. doi:10.1785/0119990151

Malagnini L, Mayeda K, Uhrhammer R, Akinci A, Herrmann RB (2007) A regional ground-motion excitation/attenuation model for the San Francisco region. Bull Seismol Soc Am 97:843–862. doi:10.1785/0120060101

Mayeda K, Walter WR (1996) Moment, energy, stress drop, and source spectra of western United States earthquakes from regional coda envelopes. J Geophys Res 101:11195–11208. doi:10.1029/96JB00112

McGuire RK (1976) EQRISK: evaluation of sites for earthquake risk. US Geological Survey, Open File Report, pp 76–67

Meghraoui M, Delouis B, Ferry M et al (2001) Active normal faulting in the upper Rhine Graben and paleoseismic identification of the 1356 Basel earthquake. Science 293(5537):2070–2073. doi:10.1126/science.1010618

Morasca P, Malagnini L, Akinci A et al (2006) Ground-motion scaling in the Western Alps. J Seismol 10(3): 315–333. doi:10.1007/s10950-006-9019-x

Musson RMW (2000) The use of Monte Carlo simulations for seismic hazard assessment in the UK. Ann Geofis 43:1–9

Musson RMW, Toro GR, Coppersmith KJ et al (2005) Evaluating hazard results for Switzerland and how not to do it: a discussion of "problems in the application of the SSHAC probability method for assessing earthquake hazards at Swiss nuclear power

plants" by J-U Klügel. Eng Geol 82(1):43–55. doi:10.1016/j.enggeo.2005.09.003
Ogata Y (1983) Estimation of the parameters in the modified Omori formula for aftershock frequencies by the maximum-likelihood procedure. J Phys Earth 31(2):115–124
Ogata Y (1999) Seismicity analysis through point-process modeling: a review. Pure Appl Geophys 155(2–4):471–507. doi:10.1007/s000240050275
Pavoni N, Maurer HR, Roth P, Deichmann N (1997) Seismicity and seismotectonics of the Swiss Alps, deep structures of the Swiss Alps, results of NRP 20. Birkhäuser, Basel, Switzerland, pp 241–250
Raoof M, Herrmann RB, Malagnini L (1999) Attenuation and excitation of three-component ground-motion in Southern California. Bull Seismol Soc Am 89:888–902
Reasenberg PA (1985) Second-order moment of Central California seismicity. J Geophys Res 90:5479–5495. doi:10.1029/JB090iB07p05479
Regenauer-Lieb K, Petit JP (1997) Cutting of the European continental lithosphere: plasticity theory applied to the present Alpine collision. J Geophys Res 102(B4):7731–7746. doi:10.1029/96JB03409
Reiter L (1990) Probabilistic seismic hazard analyses—lessons learned—a regulators perspective. Nucl Eng Des 123(2–3):123–128. doi:10.1016/0029-5493(90)90232-M
Reiter L (1991) Earthquake hazard analysis. Columbia University Press, 254 pp
Rüttener E (1995) Earthquake hazard evaluation for Switzerland, Matériaux pour la Géologie de la Suisse, Géophysique No 29 publié par la Commission Suisse de Géophysique. Schweizerischer Erdbebendienst, Zürich, p 106
Rüttener E, Egozcue JJ, Mayerrosa D, Mueller S (1996) Bayesian estimation of seismic hazard for two sites in Switzerland. Nat Hazards 14(2–3):165–178. doi:10.1007/BF00128264
Rydelek PA, Sacks IS (1989) Testing the completeness of earthquake catalogs and the hypothesis of self-similarity. Nature 337:251–253. doi:10.1038/337251a0
Rydelek PA, Sacks IS (2003) Comment on "Minimum magnitude of completeness in earthquake catalogs: examples from Alaska, the western United States, and Japan," by Stefan Wiemer and Max Wyss. Bull Seismol Soc Am 93(4):1862–1867
Sabetta F, Pugliese A (1987) Attenuation of peak horizontal acceleration and velocity from Italian strong-motion records. Bull Seismol Soc Am 77:1491–1513
Sabetta F, Pugliese A (1996) Estimation of response spectra and simulation of nonstationary earthquake ground motions. Bull Seismol Soc Am 86(2):337–352
Sägesser R, Mayer-Rosa D (1978) Erdbebengefährdung in der Schweiz. Schweizerische Bauzeitung SIA 78:3–18
Scherbaum F, Schmedes J, Cotton F (2004) On the conversion of source-to-site distance measures for extended earthquake source models. Bull Seismol Soc Am 94(3):1053–1069. doi:10.1785/0120030055
Scherbaum F, Bommer JJ, Bungum H, Cotton F, Abrahamson NA (2005) Composite ground-motion models and logic trees: methodology, sensitivities, and uncertainties. Bull Seismol Soc Am 95(5):1575–1593. doi:10.1785/0120040229
Scherbaum F, Cotton F, Staedtke H (2006) The estimation of minimum-misfit stochastic models from empirical ground-motion prediction equations. Bull Seismol Soc Am 96(2):427–445. doi:10.1785/0120050015
Schmid S, Kissling E (2000) The arc of the western Alps in the light of geophysical data on deep crustal structure. Tectonics 19(1):62–68. doi:10.1029/1999TC900057
Schmid SM, Froitzheim N, Pfiffner OA, Schonborn G, Kissling E (1997) Geophysical–geological transect and tectonic evolution of the Swiss-Italian Alps. Tectonics 16(1):186–188. doi:10.1029/96TC03723
Schnellmann M, Anselmetti FS, Giardini D, Mckenzie JA, Ward SN (2002) Prehistoric earthquake history revealed by lacustrine slump deposits. Geology 30(12):1131–1134. doi:10.1130/0091-7613(2002)030<1131:PEHRBL>2.0.CO;2
Schnellmann M, Anselmetti FS, Giardini D, Mckenzie JN, Ward SN (2004) Ancient earthquakes at Lake Lucerne. Am Sci 92(1):46–53
Schorlemmer D, Wiemer S, Wyss M (2004a) Earthquake statistics at Parkfield: 1. Stationarity of *b* values. J Geophys Res Solid Earth 109(B12):B12307.1–B12307.17
Schorlemmer D, Wiemer S, Wyss M, Jackson DD (2004b) Earthquake statistics at Parkfield: 2. Probabilistic forecasting and testing. J Geophys Res Solid Earth 109(B12):B12308.1–B12308.12
Schwarz-Zanetti G, Deichmann N, Fäh D et al (2003) The earthquake in Unterwalden on September 18, 1601: a historico-critical macroseismic evaluation. Eclogae Geol Helv 96(3):441–450
Shi Y, Bolt BA (1982) The standard error of the magnitude–frequency *b* value. Bull Seismol Soc Am 72:1677–1687
SIA (2003) Norm SIA261-Einwirkungen auf Tragwerke. Schweizerischer Ingenieur und Architekten Verein
Sissingh W (1998) Comparative tertiary stratigraphy of the Rhine Graben, Bresse Graben and Molasse Basin: correlation of Alpine foreland events. Tectonophysics 300(1–4):249–284. doi:10.1016/S0040-1951(98)00243-1
Slejko DL, Peruzza L, Rebez A (1998) Seismic hazard maps of Italy. Ann Geofis 41(2):183–214
Smit P (1996) Datenerfassung und Bestimmung der Abminderung der Bodenbewegung bei Erdbeben in der Schweiz. PhD thesis, ETH-Zurich
Sommaruga A (1999) Décollement tectonics in the Jura foreland fold-and-thrust belt. Mar Pet Geol 16:111–134. doi:10.1016/S0264-8172(98)00068-3
Strasser M, Anselmetti FS, Fäh D et al (2006) Magnitudes and source areas of large prehistoric northern Alpine earthquakes revealed by slope failures in lakes. Geology 34:1005–1008. doi:10.1130/G22784A.1

Strasser FO, Bommer JJ, Abrahamson NA (2008) Truncation of the distribution of ground motion residuals. J Seismol 12(1):79–105. doi:10.1007/s10950-007-9073-z

Taubenheim J (1969) Statistische Auswertung geophysikalischer und meteorologischer Daten, Geophysikalische Monographien, akademische Verlagsgesellschaft Geest & Portig K.-G., Leipzig

Toro GR, Abrahamson NA, Schneider JF (1997) Model of strong ground-motions from earthquakes in central and eastern North America: best estimates and uncertainties. Seismol Res Lett 6:41–57

Truffert C, Burg JP, Cazes M, Bayer R, Damotte B, Rey D (1990) Structures crustales sous le Jura et la Bresse: contraintes sismiques et gravimétriques le long des profils ECORS Bresse-Jura et Alpes II. Mem Soc Geologique Fr 156:157–164

Trümpy R (1985) Die Plattentektonik und Entstehung der Alpen. Orell Füssli, Zurich, Switzerland

Uhrhammer R (1986) Characteristics of northern and southern California seismicity. Earthq Notes 57:21

Utsu T (1999) Representation and analysis of the earthquake size distribution: a historical review and some new approaches. Pure Appl Geophys 155(2–4):509–535. doi:10.1007/s000240050276

Villemin TF, Alvarez F, Angelier J (1986) The Rhine Graben—extension, subsidence and shoulder uplift. Tectonophysics 128(1–2):47–5. doi:10.1016/0040-1951(86)90307-0

Waldhauser F, Kissling E, Ansorge J, Mueller S (1998) Three-dimensional interface modelling with two-dimensional seismic data: the Alpine crust-mantle boundary. Geophys J Int 135(1):264–278. doi:10.1046/j.1365-246X.1998.00647.x

Weichert DH (1980) Estimation of the earthquake recurrence parameters for unequal observation periods for different magnitudes. Bull Seismol Soc Am 70:1337–1346

Wells DL, Coppersmith KJ (1994) New empirical relationships among magnitude, rupture length, rupture width, rupture area and surface displacement. Bull Seismol Soc Am 84:974–1002

Wesson RL, Bakun WH, Perkins DM (2003) Association of earthquakes and faults in the San Francisco Bay area using Bayesian inference. Bull Seismol Soc Am 93(3):1306–1332. doi:10.1785/0120020085

Wiemer S, Baer M (2000) Mapping and removing quarry blast events from seismicity catalogs. Bull Seismol Soc Am 90:525–530. doi:10.1785/0119990104

Wiemer S, Wyss M (1997) Mapping the frequency-magnitude distribution in asperities: an improved technique to calculate recurrence times? J Geophys Res 102:15115–15128. doi:10.1029/97JB00726

Wiemer S, Wyss M (2000) Minimum magnitude of complete reporting in earthquake catalogs: examples from Alaska, the Western United States, and Japan. Bull Seismol Soc Am 90:859–869. doi:10.1785/0119990114

Wiemer S, Wyss M (2002) Mapping spatial variability of the frequency–magnitude distribution of earthquakes. Adv Geophys 45:259–302

Wiemer S, Wyss M (2003) Reply to "Comment on 'Minimum magnitude of completeness in earthquake catalogs: examples from Alaska, the western United States, and Japan,' by Stefan Wiemer and Max Wyss," by Paul A. Rydelek and I.S. Sacks. Bull Seismol Soc Am 93(4):1868–1871

Woo G (1996) Kernel estimation methods for seismic hazard area source modeling. Bull Seismol Soc Am 86:353–362

Wüster J (1993) Discrimination of chemical explosions and earthquakes in central Europe—a case study. Bull Seismol Soc Am 83:1184–1212

Ye S, Ansorge J, Kissling E, Mueller S (1995) Crustal structure beneath the Eastern Swiss Alps derived from seismic-refraction data. Tectonophysics 242(3–4):199–221. doi:10.1016/0040-1951(94)00209-R

Youngs RR, Swan FH, Power MS, Schwartz DP, Green RK (1987) Probabilistic analysis of earthquake ground shaking hazard along the Wasatch Front, Utah. In: Glori P-L, Hays W-W (eds) Assessment of regional earthquake hazard and risk along the Wasatch Front, Utah. US Geological Survey Open File Report, pp 1–110